Physics – Uspekhi **47** (1) 1 – 15 (2004)

REVIEWS OF TOPICAL PROBLEMS PACS numbers: **11.15.–q**, 12.38.Aw, 12.38.Lg

Vacuum, confinement, and QCD strings in the vacuum correlator method

D S Kuz'menko, V I Shevchenko, Yu A Simonov

DOI: 10.1070/PU2004v047n01ABEH001696

Contents

Abstract. QCD vacuum properties and the structure of color fields in hadrons are reviewed using the complete set of gauge-invariant gluon field correlators. QCD confinement is produced by correlators with a certain Lorentz structure, which violate the Abelian Bianchi identities and are therefore absent in QED. These correlators are used to define an effective colorless field satisfying the Maxwell equations with a nonzero effective magnetic current. In the language of correlators and the effective field, it is shown that non-Abelian interaction of gluon gauge fields leads to quark confinement due to effective circular magnetic currents that squeeze gluon fields into a string in accordance with the 'dual Meissner effect'. Distributions of effective gluon fields in mesons, baryons, and glueballs with static sources are plotted.

D S Kuz'menko, Yu A Simonov Institute of Theoretical and Experimental Physics, B. Cheremushkinskaya ul. 25, 117218 Moscow, Russian Federation
Tel. (7-095) 129 94 15. Fax (7-095) 127 08 33
E-mail: kuzmenko@heron.itep.ru, simonov@heron.itep.ru
V I Shevchenko Institute of Theoretical and Experimental Physics, B. Cheremushkinskaya ul. 25, 117218 Moscow, Russian Federation
Tel. (7-095) 129 94 15. Fax (7-095) 127 08 33
E-mail: shevchen@heron.itep.ru
Institute of Theoretical Physics, Utrecht University, Leuvenlaan 4, 3584 CE Utrecht, Netherlands
E-mail: V.Shevchenko@phys.uu.nl

Received 14 November 2002, revised 20 June 2003
Uspekhi Fizicheskikh Nauk **174** (1) 3 – 18 (2004)
Translated by D S Kuz'menko, V I Shevchenko, Yu A Simonov; edited by A M Semikhatov

1. Introduction

The QCD is a unique example of field theory lacking internal contradictions and at the same time explaining all physical phenomena in strong interactions [1, 2]. The theoretical understanding of QCD is difficult because all its basic features are of a nonperturbative nature, and the QCD vacuum is a dense and highly nontrivial substance. In fact, in modern quantum field theory, one often represents the vacuum as a specific material substance with definite characteristics directly analogous to condensed matter physics. As illustrative examples, we mention the description of the Casimir effect and relative phenomena, as well as the Higgs mechanism in the Standard Model. In the last case, one deals with the vacuum condensate of the scalar field $\langle\phi\rangle$, while quantum excitations above this condensate are considered as Higgs particles.

The nontriviality of the QCD vacuum is revealed by the fact that this medium has nonzero values of gluonic condensate [3], $\langle F^a_{\mu\nu}F^a_{\mu\nu}\rangle = (600\ \text{MeV})^4$, and of the quark condensate, $\langle\bar{q}q\rangle = -(250\ \text{MeV})^3$. As has become clear during the last decades, it is the vacuum properties which bring about confinement (see, e.g., the review [4]). For theoretical calculations in QCD, until recently one usually exploited the perturbation theory augmented by some models of nonperturbative mechanisms. The situation changed with the advent of the QCD sum rule method [3], which uses the gauge-invariant formalism of condensates to describe the nonperturbative contributions. However, this method is not sufficient for most effects at large distances, e.g., for confinement or spontaneous violation of chiral symmetry.

The systematic description of all QCD phenomena is, in principle, made possible due to the appearance of the vacuum correlator method (VCM) (see [5 – 7] and the review [8]) in which the basic elements are given by the complete set of field

correlators of the form

$$D^{(n)}_{\mu_1\nu_1\ldots\mu_n\nu_n}(x_1,\ldots,x_n,x_0) = \left\langle \mathrm{Tr}\; G_{\mu_1\nu_1}(x_1,x_0)\ldots G_{\mu_n\nu_n}(x_n,x_0)\right\rangle, \quad (1)$$

where the notation $G_{\mu_1\nu_1}(x_1,x_0)$ is used for the gluon field strength covariantly shifted along some curve [see Eqn (5)].

The basic tools of VCM are the gauge-invariant Green's functions of white objects, which can be written as path integrals through field correlators (1) using cluster expansion (see, e.g., Refs [9, 10]). A question may arise at this point: why do we consider only white (i.e., gauge-invariant) objects in VCM and not, for example, propagators in some fixed gauge? The answer is tightly connected to the difference between gauge invariance in Abelian and non-Abelian theories.

In the Abelian theory, e.g., in QED, the requirement of gauge invariance does not forbid us from considering the problems with formally gauge-noninvariant asymptotic states, like electron – electron scattering. The gauge invariance of the cross section occurs in this case due to the conservation of the Abelian current. In the non-Abelian theory with confinement, like QCD, the situation is different and the problem of scattering of isolated quarks makes no sense.

Beyond perturbation theory, the strong interaction causes pair creation at large distances and renders the problem essentially multi-particle. In QCD, one usually considers quark – quark scattering for quarks inside white objects (i.e., described by gauge-invariant functions), such as hadrons. The same is true for the problems connected with the spectrum of bound states: in QED, the problem of a neutral atom spectrum is not fundamentally different from the problem of the spectrum of a charged ion, but in QCD, an analog of the last problem has no meaning.

Therefore, the set of correlators (1) can be considered a starting dynamical basis yielding a phenomenological gauge-invariant description of physical processes. But the actual situation is much more interesting. First of all, the lattice calculations give important evidence that the first nontrivial correlator with $n = 2$ already dominates, and the total contribution of all the highest correlators is below a few percent (see review [11]). As shown in Refs [6, 7], the lowest (or Gaussian, [1] as it is called in what follows) correlator can be expressed through two scalar form factors $D(x_1 - x_2)$ and $D_1(x_1 - x_2)$.

Second, the form factors $D(x_1 - x_2)$ and $D_1(x_1 - x_2)$ have been measured in the lattice calculations and have nonperturbative parts of exponential shape with a characteristic small correlation length λ. Finally, the function $D^{(2)}$ [and therefore also $D(x_1 - x_2)$ and $D_1(x_1 - x_2)$] are directly connected to the Green's functions of the so-called glue-lumps [12 – 14]. The latter can be calculated analytically in terms of the only QCD mass scale, e.g., through the string tension σ and the coupling constant α_s. Thus, the formulation of the nonperturbative dynamics in QCD turns out to be self-consistent and one should additionally calculate λ through σ, which was done earlier in Ref. [15], and also connect σ and Λ_{QCD} and write the explicit form of correlators $D^{(n)}$. In this way, one would also be able to understand the dominance of $D^{(2)}$ analytically (one can find the first results in this direction in Refs [16, 17]).

[1] We use the analogy with the so-called Gaussian, or white, noise described by a quadratic correlator, in this case with vanishing correlation length.

On the other hand, the formalism of field correlators is to a large extent unusual to physicists brought up in the standard lore of perturbative, or even more so, Abelian gauge theory. In the context of the confinement problem, such a 'linear' Abelian approach is realized in the so-called 'dual Meissner scenario', which contains a simple qualitative picture of the confinement mechanism in QCD [18, 19]. In this approach, the charges (quarks) and the monopole medium play an active role, filling the vacuum.

Many lattice and analytic studies (see, e.g., Refs [20 – 23]) demonstrate that the string formation between quark and antiquark is connected in this picture with the appearance of circular monopole currents $\mathbf{k}$ around the string, which obey the dual Ampere law $\mathbf{k} = \mathrm{rot}\,\mathbf{E}$. From the physical standpoint, this situation is similar to the Meissner effect in the standard superconductivity phenomenon, modulo interchange of the effective electric and magnetic charges.

The main problem of this picture is that the very notion of the magnetic monopole cannot be exactly defined in QCD. This arbitrariness can be seen, first of all, in the gauge dependence of the monopole definition, and second, in the difficulties with the continuum limit for the lattice monopoles, defined by the flux through an elementary cube. There exist numerous publications with different suggestions on how to deal with this problem (see, e.g., Ref. [24]).

While confinement properties are studied on the lattice numerically, (in particular, using the Abelian projection), they are also an object of investigation in the effective Lagrangian approach and in different dielectric vacuum models of QCD [25 – 34]. The basic field theory problem is then replaced by a classical variational problem for the effective Lagrangian, which yields a system of differential equations, to be solved numerically. In this way, one introduces an effective dielectric constant of the vacuum, depending on the effective fields and ensuring quark confinement.

Using the field correlator method as a universal language, one can define gauge-invariant (with respect to the gauge symmetry of the original non-Abelian theory) effective field $\mathcal{F}_{\mu\nu}(x)$.This generalizes the Makeenko – Migdal field [35] (see also Ref. [36]) for an arbitrary position of a point x with respect to the Wilson loop. The effective electric field near the charge turns out to be the gradient of the color-Coulomb potential, and in the case of the Abelian theory, $\mathcal{F}_{\mu\nu}(x)$ is the standard field strength.

The effective field satisfies the Maxwell equations, where the right-hand side involves the electric current j_μ and the magnetic current k_μ. The source of k_μ is primarily the triple correlator of the form $\langle EEB\rangle$ (as was already found in Ref. [4]) describing the emission of the color-magnetic field by the color-electric; the latter can be visualized as the emission of the color-magnetic field by an effective magnetic charge (monopole). In the language of field correlators, one can easily demonstrate that the system of equations for the effective fields describes the QCD string and the circular magnetic currents around it. In this way, the picture of the dual Meissner effect is reproduced in gauge-invariant terms.

With the help of $\mathcal{F}_{\mu\nu}$, one can investigate the structure of the QCD string in detail. The first computations of the string profile in Ref. [37] have agreed well with the results calculated via $D(x^2), D_1(x^2)$ and those obtained independently on the lattice. The subsequent study of the string structure [38] has shown an interesting phenomenon of the profile saturation,

where the profile (i.e., the field distribution across the string) does not change for sufficiently long strings. The pattern of the baryon field has turned out to be even more interesting. Baryons and, to be more precise, nucleons are the basis of the bulk of stable matter around us. The physical problem of the structure of the baryon field is especially interesting from both theoretical and practical standpoints.

Two types of baryon field configurations were discussed in the literature: with the string junction in the middle (the Y-shape) and of a triangular shape (the Δ-shape). Using the vacuum correlator method, the baryon configuration was computed analytically in Refs [39, 40], where the presence of the string junction in the field distribution was explicitly demonstrated, thereby excluding the Δ-type configuration. On the other hand, the latter is possible for the three-gluon glueballs, and the corresponding field was calculated in Ref. [40]. One should mention that these baryon field distributions are also in agreement with the lattice calculations using the Abelian projected QCD [41] (see also the review paper of Bornyakov et al. [42]).

Three valence gluons act as field sources in three-gluon glueballs. The field structure of these systems has some specific features and can be of both types, the Δ-type (unlike baryons) and the Y-type (like baryons), and its study helps us to better understand the physics of confinement. In addition, the three-gluon glueballs are connected with the processes of the odderon exchange (i.e., the glueball exchange with odd charge parity), and are therefore also interesting from the experimental standpoint. In what follows, in addition to the effective field distributions, we therefore also discuss the W-loops and the static potentials of baryons and three-gluon glueballs.

The paper has the following structure. In Section 2, the discussion of field correlator properties in QCD is given, and in particular, the important phenomenon of the Casimir scaling is explained. In Section 3, the effective field $\mathcal{F}_{\mu\nu}$ and the currents j_μ, k_μ are introduced and the dual Meissner effect is studied. The problem of the total string energy and other approaches to it are also discussed at the end of this section. In Section 4, the static potentials and field distributions in baryons and three-gluon glueballs with static sources are given. The main results are summarized and some perspectives are outlined in the conclusion. [2]

Everywhere in what follows, unless especially stressed otherwise, the Euclidean metric is used with the notation $k = (k_1, k_2, k_3, k_4)$ for 4-vectors and $kp = k_\mu p^\nu \delta_\nu^\mu$ for scalar products. Three-dimensional vectors are denoted as $\mathbf{k} = (k_1, k_2, k_3)$ and the Wick rotation corresponds to the replacement $k_4 \to \mathrm{i}k_0$.

2. Properties of QCD vacuum in gauge-invariant approach

2.1 Definition of the basis of gauge-invariant correlators

The following remark must be made before we proceed. There is an important difference between pure Yang–Mills theory (gluodynamics) and QCD, namely, the latter contains dynamic fermions, in particular light u and d quarks. This circumstance plays no crucial role in the description of confinement because gluodynamics confines color as QCD does, which is supported by direct lattice calculations (see, e.g., Ref. [43]) and different qualitative arguments. In most cases, we therefore consider the pure Yang–Mills theory in this review, while quarks play the role of external sources.

One of the main objects in gauge theory is the Wilson loop [45, 46], which we define as

$$W(C) = P\exp\left(\mathrm{i}g\oint\limits_C \mathrm{d}z_\mu\, A_\mu^a(z) t^a\right). \tag{2}$$

Here, t^a are the generators in some given representations of the gauge group. The Wilson loop defines an external current J that corresponds to a point particle charged according to the chosen representation and moving along the closed contour C.

The phase factor for a nonclosed curve connecting points x and y is given by

$$\Phi(x;y) = P\exp\left(\mathrm{i}g\int_x^y \mathrm{d}z_\mu\, A_\mu^a(z) t^a\right). \tag{3}$$

Under gauge transformations, we have

$$\Phi(x;y) \to \Phi^U(x;y) = U^\dagger(x)\,\Phi(x;y)\,U(y)\,. \tag{4}$$

This implies that the trace $\mathrm{Tr}\, W(C)$ is gauge-invariant. [3] We normalize Tr everywhere as $\mathrm{Tr}\,\mathbf{1}_d = 1$ for the given representation of dimension d.

Using definition (3), we introduce $G_{\mu\nu}(x, x_0)$ as

$$G_{\mu\nu}(x, x_0) = \Phi(x_0; x)\, F_{\mu\nu}(x)\, \Phi(x; x_0)\,, \tag{5}$$

where $F_{\mu\nu} = \partial_\mu A_\nu - \partial_\nu A_\mu - \mathrm{i}g[A_\mu A_\nu]$ is the non-Abelian field strength and the curve connecting the points x and x_0 does not self-intersect. In Abelian theory, $G_{\mu\nu}(x, x_0) \equiv F_{\mu\nu}(x)$, but in Yang–Mills theory, $G_{\mu\nu}(x, x_0)$ and $F_{\mu\nu}(x)$ transform differently under gauge transformations, as is clear from (4). We can now construct vacuum averages of the products of $G_{\mu\nu}(x_n, x_0)$ as

$$D^{(2)}_{\mu\nu\rho\sigma}(x, y, x_0) = \left\langle \mathrm{Tr}\, G_{\mu\nu}(x, x_0)\, G_{\rho\sigma}(y, x_0)\right\rangle, \tag{6}$$

$$D^{(3)}_{\mu\nu\rho\sigma\alpha\beta}(x, y, z, x_0) = \left\langle \mathrm{Tr}\, G_{\mu\nu}(x, x_0)\, G_{\rho\sigma}(y, x_0)\, G_{\alpha\beta}(z, x_0)\right\rangle \tag{7}$$

and similarly for higher orders. Correlators (6) and (7) are gauge-invariant, but nonlocal — expressions (6) and (7) depend on the position of the points x, y, and z as well as on the position of the point x_0 and the contour profile used in (5).

Physical observables such as the Wilson loop vacuum average and static potential or the effective field extracted from it, as well as Green's functions of colorless states, are independent of x_0 and contour profiles when all the correlators $D^{(n)}$, $n \geqslant 2$ are taken into account. This is not true, however, if one takes only the lowest $n = 2$ term. In this case, it is convenient to minimize the corresponding dependence (and hence the contribution of higher correlators), choosing x_0 and the contours corresponding to the minimal surface. This is similar to what one usually does in perturbation theory, minimizing the contribution of omitted terms by

[2] The ideas on which this review is based were partly reported by one of the authors (Yu S) in his plenary talk at the conference dedicated to the 90th anniversary of I Ya Pomeranchuk's birthday.

[3] In the literature, the trace is often included in the definition of the Wilson loop.

the proper choice of the subtraction point μ, of which the exact answer should be independent.

2.2 Computation of the Wilson loop and Green's functions in terms of correlators

Speaking in general terms, each function $D^{(n)}$ is itself an important characteristic of the vacuum structure in a given gauge theory. What is more important, however, is the possibility to express the Wilson loop average in terms of correlators (6) and (7). Indeed, Stokes's theorem (or, more precisely, its non-Abelian generalization [47 – 52]) leads to

$$\left\langle \operatorname{Tr} W(C)\right\rangle = \left\langle \operatorname{Tr}\mathcal{P}\exp\left(\mathrm{i}g\int_S \mathrm{d}\sigma_{\mu\nu}(z)\, G_{\mu\nu}(z,x_0)\right)\right\rangle = \exp\sum_{n=2}^{\infty}(\mathrm{i})^n\,\Delta^{(n)}[S]\,. \tag{8}$$

We have used cluster expansion to exponentiate the series in correlators at the final stage (see, e.g., Refs [53, 54]).

Integral moments $\Delta^{(n)}[S]$ over the surface S of *irreducible* correlators, known as cumulants in statistical physics, can be expressed as linear combinations of the integrals of the correlators $D^{(n)}$. For example, for a two-point correlator, we have

$$\Delta^{(2)}[S] = \frac{1}{2}\int_S \mathrm{d}\sigma_{\mu\nu}(z_1)\int_S \mathrm{d}\sigma_{\rho\sigma}(z_2)\, g^2 D^{(2)}_{\mu\nu\rho\sigma}(z_1,z_2,x_0)\,. \tag{9}$$

For higher terms, the ordering is important (see, e.g., Ref. [16], where exact computations for $n = 4$ are performed).

Expression (8) is of central importance for the discussed formalism. We now consider the propagation of a spinless particle with mass m, carrying a fundamental color charge ('quark') in the field of an infinitely heavy 'antiquark' [9, 10]. The corresponding gauge-invariant Green's function is given by

$$\mathcal{G}(x,y) = \left\langle \phi^{\dagger}(x)\,\Phi(x;y)\,\phi(y)\right\rangle, \tag{10}$$

where the quark field is denoted by $\phi(x)$.

It can be shown that $\mathcal{G}(x,y)$ admits the Feynman – Schwinger representation

$$\mathcal{G}(x,y) = \int_0^{\infty}\mathrm{d}s\int_{z_\mu(0)=x_\mu}^{z_\mu(s)=y_\mu}\mathcal{D}z_\mu \times\exp\left[-m^2 s-\frac{1}{4}\int_0^s \mathrm{d}\tau\left(\frac{\mathrm{d}z_\mu(\tau)}{\mathrm{d}\tau}\right)^2\right]\left\langle \operatorname{Tr} W(C)\right\rangle, \tag{11}$$

where the closed contour C is formed by the quark trajectory $z_\mu(\tau)$ and that of the antiquark (the latter is nothing but a straight line connecting the points x and y). We have taken the spinless case here as the simplest illustrative example; for real physical problems with spinor quark fields, there is a systematic way of analyzing spin effects [9, 10, 55]. The problem of the two-body meson or three-body baryon state can be addressed in a completely analogous way.

In all cases, the Green's function, which in principle contains full information about the mass spectrum and wave functions of the system, can be rewritten in terms of the path integrals of the Wilson loops, where the latter are expressed via correlators as in (8). Therefore, the set of correlators $D^{(n)}$ provides rich and, more importantly, universal dynamic information that one can use to compute different nonperturbative effects.[4] We stress once again that correlator (6) is itself related to the Green's function of gluon excitation in the field of an infinitely heavy adjoint source — known as a gluelump in the literature [14].

Coming to the practical side of the problem, it is natural to ask what the actual behavior of correlators (6) and (7) is and how information about it can be gained. This question is simple to answer in perturbation theory because each $D^{(n)}$ is given by a perturbative series (see, e.g., Refs [56, 57]). There are a few ways to proceed beyond perturbation theory. The first is to find nonperturbative solutions to the so-called BBGKI equations, relating the correlators of different orders [61]. This method has brought no essential progress up to now.

Another analytic strategy suggests computing correlators in terms of gluelump Green's functions [14, 15]. The third and most successful way is to study the problem on the lattice. There are quite a few sets of numerical data [62 – 66], which we discuss below. It is obvious, however, that numerical results concerning one or a few particular correlators (for example, the lowest one) are useless if the general properties of the whole ensemble are unknown. To discuss them, we return to expression (8).

2.3 Gaussian dominance

It has already been stressed that the price we have paid for manifest gauge-invariance of (8) is the dependence of (6) and (7) on the contour profiles entering $\Phi(x;y)$. These contours are, generally speaking, arbitrary nonselfintersecting curves or, better to say, they can be freely chosen in some (large enough) set. As a result, the quantities $\Delta^{(n)}[S]$ in (8) depend on this choice, while $W(C)$ is obviously independent of S. The contradiction is spurious and one can demonstrate that this contour dependence is canceled in the total sum, despite its presence in each individual summand $\Delta^{(n)}[S]$. In this sense, the choice of the surface S in (8) [corresponding to the choice of integration contours in the correlators $D^{(n)}$ in Stokes's theorem] is free, as it should be.

We can take a different attitude and assume that the problem involves a physically distinguished surface. What is then the hierarchy of cumulants $\Delta^{(n)}[S]$ on this surface? This question is of general interest, but it also has important practical meaning — in many specific problems, a surface singled out for some physical reasons can easily be found. For a single Wilson loop, it is given by the minimal-area surface bounded by the contour. In the more complicated case of interacting loops [67], the surface corresponding to the minimal energy of the system can be taken.

In any case, two different scenarios are distinguished: in the case where

$$\Delta^{(2)}[S] \gg \Delta^{(n)}[S] \quad \text{for} \quad n>2\,, \tag{12}$$

the ensemble of correlators (and the vacuum of the theory) is called *stochastic*; in the case where (12) does not hold (for example, all cumulants are of the same order), the ensemble of correlators is called *coherent*. The general framework described in this review takes the effects of all cumulants into account but, as should be clear, it shows its strong sides in

[4] The discussed formalism can be applied in perturbation theory [59] as well. In this context, it allows us to sum up a perturbative subseries, which gives the well-known 'Sudakov form factor' as a result of the first approximation (see [60] and [10] and references therein).

theories with the stochastic vacuum. The lowest two-point Gaussian cumulant (9) is dominant in the stochastic ensemble, while higher-order terms can be considered small corrections. This situation is known as Gaussian dominance.

Is the QCD vacuum stochastic or coherent? To answer this question in a straightforward way, one has to compute (for example, numerically on the lattice) different cumulants and verify criterion (12) for them. Unfortunately, this research program is too intricate for modern lattice technologies and almost all actual results are obtained for Gaussian cumulants only. There is important indirect evidence, however, supporting the idea that the Yang–Mills vacuum is indeed stochastic and not coherent in the sense of (12). Of prime importance in this context is the Casimir scaling phenomenon [68–71] (see also Refs [72–75]).

Using (8) and taking the well-known relation between static potential and Wilson loop average into account, one can obtain, assuming Gaussian dominance, that

$$V(R) = \lim_{T\to\infty} \frac{1}{T}\,\Delta^{(2)}[S = R\times T]\,. \tag{13}$$

In accordance with definitions (6) and (9), we then have $V(R) \sim C_d$, where the eigenvalue of the Casimir operator in the representation d is given by $\delta_{ab}t^a t^b = C_d\cdot \mathbf{1}_d$. We recall that the representation of the Lie group SU(N) of dimension d is characterized by N^2-1 generators t^a, which can be realized as $d\times d$ matrices commuting as $[t^a t^b] = if^{abc}t^c$. Proportionality of the static potential to C_d is called the Casimir scaling and was first discussed in Ref. [76].

It can be easily shown that contributions from higher cumulants to static potential (13) are, generally speaking, not proportional to C_d (although they can contain terms linear in C_d). Therefore, a good accuracy (deviation not exceeding 5%) of the Casimir scaling demonstrated on the lattice is a serious argument in favor of Gaussian dominance.

Moreover, attempts to reproduce the Casimir scaling in many other models of nonperturbative QCD vacuums encounter serious difficulties [11, 77, 78]. Another argument, which is not directly related to the previous one, is that the radius of the confining string between quarks is independent of their non-Abelian charge (i.e., of representation d) [79]. These results would look like fine-tuning effects without Gaussian dominance. It is also worth mentioning that 'vacuum state dominance' successfully used for years in the QCD sum-rule formalism is nothing but Gaussian dominance in our language.

2.4 Structure of two-point correlators

We have mentioned the relation between the correlators $D^{(n)}$ and the gluelump Green's functions. For the simplest Gaussian correlator (6), this can be seen clearly if the contours are straight lines and the points x, y, and x_0 belong to one and the same line. The correlator then depends on the only variable $z = x - y$ and can be represented as

$$D^{(2)}_{\mu\nu\rho\sigma}(z) = \left\langle F^a_{\mu\nu}(0)\, P\exp\left(\mathrm{i}g\int_0^1 \mathrm{d}s\, z_\mu\, A^b_\mu(sz)\, f^{abc}\right) F^c_{\rho\sigma}(z)\right\rangle . \tag{14}$$

Expression (14) contains the phase factor in the adjoint representation (to be compared with the previous formulas where we worked with fundamental phase factors, i.e., with $N\times N$ matrices), which makes its physical content self-evident. Namely, the gauge-invariant function $D^{(2)}(z)$ describes gluon propagation in the field of an infinitely heavy adjoint charge, fully analogous to the fundamental case [compare (10) and (14)]. The choice $z = (\mathbf{0}, T)$ corresponds to the static source at the origin.

The confining string worldsheet given by the surface S in (8) interacts with itself by one-gluelump or many-gluelump exchanges. This interaction depends on the profile of S such that the total answer for the Wilson loop average is S-independent. Qualitatively, Gaussian dominance occurs when this 'gluelump gas' becomes 'ideal' for some particular surface in the sense that the integral contribution of higher cumulants $\Delta^{(n)}$, $n > 2$, is small on this surface. This also means that two-gluon gluelumps weakly interact with each other. The deviation from the Casimir scaling (which, as we have already noticed, is small) can be expressed in terms of irreducible averages of the gauge-invariant operators $\langle \mathrm{Tr}\,(\mathcal{O}_1)\,\mathrm{Tr}\,(\mathcal{O}_2)\rangle$ describing interaction of gluelumps [16]. In particular, this implies that such deviation is suppressed in a large N limit.

To avoid misunderstanding, we stress that gluelumps do not exist as physical particles in the spectrum of the theory. It would also be wrong to interpret (14) in terms of a 'massive gluon'. In a limited sense, gluelumps are analogous to Kalb–Ramond fields that describe dual vector bosons and play an important role in constructing string representations of compact QED [36] and the Abelian Higgs model [80] (see also [81, 82]). The discussed picture with the gluelump ensemble on the worldsheet makes sense only in the presence of an external current forming the Wilson loop (and the corresponding surface). On the other hand, correlator (14) may be studied as it is, with no reference to any external source. These studies, as mentioned above, have been successfully undertaken on the lattice.

Before we discuss actual numerical results, it is useful to represent (14) in terms of the two invariant form factors $D(z^2)$ and $D_1(z^2)$ [5–7],

$$g^2 D^{(2)}_{\mu\nu\rho\sigma}(z) = (\delta_{\mu\rho}\delta_{\nu\sigma} - \delta_{\mu\sigma}\delta_{\nu\rho})D(z^2) + \frac{1}{2}\left(\frac{\partial}{\partial z_\mu}(z_\rho\delta_{\nu\sigma} - z_\sigma\delta_{\nu\rho}) - \frac{\partial}{\partial z_\nu}(z_\rho\delta_{\mu\sigma} - z_\sigma\delta_{\mu\rho})\right) D_1(z^2)\,. \tag{15}$$

Confinement (the linear potential between a static quark and an antiquark in the fundamental representation) occurs in the Gaussian dominance picture when $D(z^2)$ does not vanish.

Indeed, at large distances, it follows from (9) and (13) that the static potential $V(R)$ and string tension σ are given by

$$V(R) = \sigma R + \mathcal{O}(R^0)\,, \qquad \sigma = \frac{1}{2}\int \mathrm{d}^2 z\, D(z^2)\,. \tag{16}$$

The perturbative contribution dominates at small distances [56, 57]. The nonperturbative part of the correlator is usually represented as

$$D(z^2) \sim \exp\left(-\frac{|z|}{\lambda}\right). \tag{17}$$

This exponential fit is in very good agreement with lattice data at sufficiently long distances. The situation with the nonperturbative component of the form factor $D_1(z^2)$ is less clear numerically: one can fit this function with or without the

nonperturbative part equally well. In the rest of this paper, we use D_1 with no nonperturbative part.

It is important that from a practical standpoint (for hadron spectrum computation, for example) one has no need to know the detailed profile of the form factors $D(z^2)$ and $D_1(z^2)$: physical quantities are determined mostly by the string tension σ. The quantity λ is known as the correlation length of the QCD vacuum: as is clear from our discussion, this quantity is nothing but the inverse mass of the lowest gluelump, $\lambda = 1/M$. On the other hand, the typical size of the vacuum domain where fields are correlated is given by the same λ [83]. The physics of nonlocality switches on at distances larger that λ and has many phenomenological manifestations. One of the most interesting (the confining string formation) is discussed in what follows. We use the numerical value $\lambda = 0.2$ fm in accordance with the lattice results.

So far, we have not mentioned the problem of deconfinement. There are basically two groups of physically interesting questions related to this problem. The first covers dynamic aspects of the confinement – deconfinement phase transition. The second group deals with symmetric properties of the vacuum in different phases. In the context of our discussion, a typical question from the first group is as follows: what does temperature deconfinement phase transition correspond to in terms of correlators? The second group provides questions like: where is screening of zero N-ality charges at large distances hidden in expression (8)? We have no possibility to discuss these important issues in the present review and refer the reader to the original literature and the references therein (see Refs [4, 8, 84, 87]).

3. Mechanism of confinement and dual Meissner effect

3.1 Definition of effective fields

The formalism considered so far allows expanding Wilson loop (8) and static potential (13) over the full set of field correlators (6), (7), (15), and (17) in the whole range of distances. [5] It is well-known that the static potential at small quark – antiquark distances $r \ll \Lambda_{\rm QCD}$ in the Born approximation of perturbation theory has the form

$$V^{\rm c}(r) = -\frac{C_{\rm F}\alpha_{\rm s}}{r}\,, \tag{18}$$

where $C_{\rm F} = 4/3$ is the quadratic Casimir operator in the fundamental representation. The color factor $C_{\rm F}$ is the only difference between this potential and the Coulomb one in electrodynamics. It is therefore natural to introduce the field

$$\mathcal{E}^{\rm c} = -\nabla V^{\rm c}(r)\,, \tag{19}$$

which has the meaning of the force acting on the quark. It is obvious that (19) is valid only at small distances in the perturbation theory domain.

We define the effective gauge-invariant field that coincides with (18) and (19) at small distances,

$$\mathcal{F}^J_{\mu\nu}(x) = \big(\langle {\rm Tr}\, W(C)\rangle\big)^{-1}\big\langle {\rm Tr}\,\big({\rm i}g\, G_{\mu\nu}(x,x_0)\, W(C)\big)\big\rangle\,. \tag{20}$$

[5] The results in Section 3 are partly presented in Ref. [86].

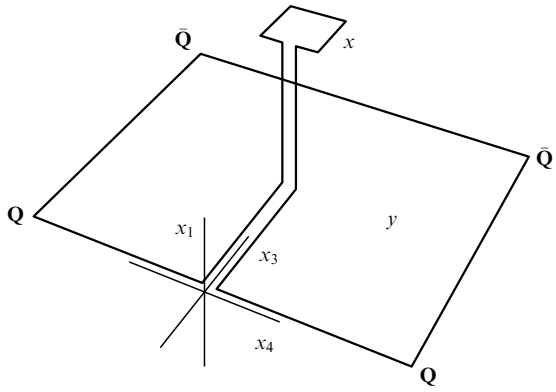

Figure 1. A connected probe (21) for a static quark and antiquark.

The superscript J stresses that the field $\mathcal{F}^J_{\mu\nu}(x)$ is a functional of the external current J corresponding to the Wilson loop $W(C)$ and, in particular, that it vanishes if $J = 0$.

The effective field can be rewritten using the *connected probe*

$$W(C, C_P) = W(C_P, x)\, \Phi(x, x_0)\, \Phi(x_0, z)\, W(C, z) \times \Phi(z, x_0)\, \Phi(x_0, x)\,, \tag{21}$$

i.e., the Wilson loop with a contour consisting of a (small) probe contour C_P connected with the contour C along some trajectory going through the point x_0. This quantity depends on the position of the 'reference point' x_0 and on the shape of the trajectory connecting C and C_P. We choose the trajectory going along the shortest path from the point x to the minimal surface of the Wilson loop (Fig. 1).

For a probe contour C_P with an infinitesimal surface $\delta\sigma_{\mu\nu}$, the effective field can be written as

$$\mathcal{F}^J_{\mu\nu}(x)\, \delta\sigma_{\mu\nu}(x) = \big\langle {\rm Tr}\, W(C)\big\rangle^{-1}\big(\big\langle {\rm Tr}\, W(C, C_P)\big\rangle - \big\langle {\rm Tr}\, W(C)\big\rangle\big) \equiv \tilde{M}(C, C_P)\,. \tag{22}$$

In particular, if the probe contour has a size $a \times a$, the electric field is expressed as

$$\mathbf{n}\cdot\boldsymbol{\mathcal{E}}^J(x) = \frac{\tilde{M}(C, C_P)}{a^2}\,, \tag{23}$$

where $\mathbf{n}$ is the unit vector defining the orientation of the probe contour in coordinate space. In this context, we note the expression for the moment of forces acting on the frame with the electric current I in the magnetic field $\mathbf{B}$, known from general physics. Namely, when the frame is oriented in the plane $(\mathbf{n}^{(1)}, \mathbf{n}^{(2)})$ and $\mathbf{n}^{(1)}$ is chosen orthogonal to the magnetic field, the moment of acting forces M takes the form

$$\mathbf{n}^{(2)}\cdot\boldsymbol{\mathcal{B}} = \frac{M}{a^2}\,, \qquad \boldsymbol{\mathcal{B}} \equiv I\mathbf{B}\,. \tag{24}$$

Comparing this relation with (23), we see that $\tilde{M}(C, C_P)$ defined in (22) has the interpretation of the 'dual' moment of acting forces.

3.2 Definition of effective currents

We recall that in electrodynamics, $G_{\mu\nu}(x, x_0) \equiv F_{\mu\nu}(x)$ and equation (20) defines the classical field distribution deter-

mined by the external electric current

$$g^2 J_\mu(x) = g^2 \int_C \mathrm{d}z_\mu \, \delta^{(4)}(z-x)$$

(where g denotes the electric charge) and satisfying the corresponding Maxwell equations.

Using the differential relations for phase factors (see, e.g., Refs [47–52]), we can formally write the 'effective electrodynamics' equations

$$\frac{1}{2}\,\epsilon_{\mu\rho\alpha\beta}\,\frac{\partial}{\partial x_\rho}\,\mathcal{F}^J_{\alpha\beta}(x) = k^J_\mu(x)\,, \qquad \frac{\partial}{\partial x_\rho}\,\mathcal{F}^J_{\rho\mu}(x) = j^J_\mu(x) \tag{25}$$

for the field $\mathcal{F}^J_{\mu\nu}(x)$ defined by (20). The superscript J indicates, as before, that the 'electric' current j^J_μ and the 'magnetic' current k^J_μ are functionals of the external current J,

$$\begin{aligned} j^J_\nu(x) &= \big(\big\langle \mathrm{Tr}\, W(C)\big\rangle\big)^{-1} \\ &\quad\times \big\langle \mathrm{Tr}\,\big(\Phi(x_0;x)\,\mathrm{i}gD_\mu F_{\mu\nu}(x)\,\Phi(x;x_0)\,W(C)\big)\big\rangle \\ &\quad + g^2\big(\big\langle \mathrm{Tr}\, W(C)\big\rangle\big)^{-1}\int_0^1 \mathrm{d}s\,\frac{\partial u_\alpha(s,x)}{\partial s}\,\frac{\partial u_\beta(s,x)}{\partial x_\mu} \\ &\quad\times \big\langle \mathrm{Tr}\,\big[G_{\mu\nu}(x,x_0), G_{\alpha\beta}(u,x_0)\big]\,W(C)\big\rangle\,, \end{aligned} \tag{26}$$

$$\begin{aligned} k^J_\nu(x) &= g^2\big(\big\langle \mathrm{Tr}\, W(C)\big\rangle\big)^{-1}\int_0^1 \mathrm{d}s\,\frac{\partial u_\alpha(s,x)}{\partial s}\,\frac{\partial u_\beta(s,x)}{\partial x_\mu} \\ &\quad\times \big\langle \mathrm{Tr}\,\big[\tilde{G}_{\mu\nu}(x,x_0), G_{\alpha\beta}(u,x_0)\big]\,W(C)\big\rangle\,. \end{aligned} \tag{27}$$

The integration contour in (26) and (27) is determined by the function $u_\mu(s,x)$ with the boundary conditions $u^\mu(0,x) = x^\mu_0$, $u_\mu(1,x) = x_\mu$ and the square brackets denote commutators in color indices. Equations (26) and (27) define effective currents that satisfy (25) and (20) identically. But the non-Abelian Bianchi identities $D_\mu \tilde{F}_{\mu\nu}(x) = 0$ respecting the gauge nature of QCD have been used in deriving (27). It is obvious that both electric and magnetic effective currents are conserved because the tensor $\mathcal{F}_{\mu\nu}$ is anti-symmetric.

If the gauge coupling is small, we can use the equation of classical gluodynamics,

$$\mathrm{i}gD_\mu F^a_{\mu\nu} = g^2 J^a_\nu\,, \qquad J^a_\mu(x) = J_\mu(x)T^a \tag{28}$$

for the electric current in (26), with

$$J_\mu(x) = \int_C \mathrm{d}z_\mu\,\delta^{(4)}(z-x)\,.$$

The second term in (26) does not contribute to the leading order in the gauge coupling constant $\alpha_\mathrm{s} = g^2/(4\pi)$, and the expression for the electric current becomes

$$j^J_\nu(x) = 4\pi C_\mathrm{F}\alpha_\mathrm{s}\,J_\nu(x) \tag{29}$$

[the fundamental Casimir operator $C_\mathrm{F}\hat{1} = T^aT^a = (4/3)\hat{1}$], i.e., it has the form of a classical current of electrodynamics. In the particular case of a static quark and antiquark, this becomes the Gauss law for a color Coulomb field.

We note that because the first term (the unity) in the expansion of the Wilson loop $W(C)$ in powers of the field does not contribute to (27) (the trace of a commutator vanishes), the first nontrivial contribution to $k^J_\mu(x)$ is proportional to the non-Abelian field strength correlator of the third order. Therefore, up to higher correlators, the magnetic current is proportional to the correlator $\langle E^a_i B^b_j E^c_k\rangle f^{abc}\epsilon_{ijk}$, and hence the effective magnetic current emerges due to the non-Abelian emittance of the color-magnetic field by the color-electric one. The same structures in the expression for the electric current are responsible for vacuum polarization (see discussion in Section 3.5).

3.3 Effective field distribution in two-point approximation

We consider a rectangular Wilson loop of a static quark and antiquark. According to the hypothesis of bilocal (Gaussian) dominance supported by Casimir scaling (see Section 2.3), the dominant contribution to the Wilson loop average is given by two-point correlator (6) and (15). Therefore, in calculating effective field distributions below, we restrict ourselves to the contribution of the two-point correlator, assuming that the contribution of the other correlators is inessential for confinement description. The expression for the effective field then takes the form

$$\mathcal{F}_{\mu\nu}(x) = \int_S \mathrm{d}\sigma_{\alpha\beta}(y)\,g^2 D^{(2)}_{\alpha\beta\mu\nu}(x-y)\,, \tag{30}$$

where $y \in S$ (S is the minimal surface of the Wilson loop) and the bilocal correlator $D^{(2)}$ is defined in (15).

We let $\mathbf{n} = \mathbf{R}/R$ denote the unit vector directed from the quark to the antiquark and rewrite (30) as

$$\mathcal{F}_{\mu\nu}(x) = \int_S \mathrm{d}^2 y\ \mathrm{Tr}\,\big\langle gF_{\mu\nu}(x)\,\Phi(x,y)\,\mathbf{n}g\mathbf{E}(y)\,\Phi(y,x)\big\rangle\,, \tag{31}$$

which clearly indicates that the magnetic field $\mathcal{B}$ is absent. The substitution of parameterization (15) in (31) yields the expression for the effective electric field

$$\mathcal{E}_i(\mathbf{r},\mathbf{R}) = n_k\int_0^R \mathrm{d}l\int_{-\infty}^{\infty}\mathrm{d}t\left(\delta_{ik}D(z) + \frac{1}{2}\,\frac{\partial z_i\,D_1(z)}{\partial z_k}\right), \tag{32}$$

where $z = (\mathbf{r} - \mathbf{n}l, t)$.

The perturbative part of the field corresponding to the contribution of the form factor D_1 to field (32) can be represented in the Born approximation as the difference

$$\boldsymbol{\mathcal{E}}^{D_1}(\mathbf{r}) = \boldsymbol{\mathcal{E}}^\mathrm{c}(\mathbf{r}) - \boldsymbol{\mathcal{E}}^\mathrm{c}(\mathbf{r}-\mathbf{R})\,. \tag{33}$$

According to (18) and (19), the field

$$\boldsymbol{\mathcal{E}}^\mathrm{c}(\mathbf{r}) = \frac{C_\mathrm{F}\alpha_\mathrm{s}\mathbf{r}}{r^3}\,. \tag{34}$$

The corresponding form factor given by

$$D_1^{(\mathrm{p})}(z) = \frac{4C_\mathrm{F}\alpha_\mathrm{s}}{\pi z^4} \tag{35}$$

can also be calculated directly in perturbation theory [89].

It was discussed in Section 2 that confinement follows from the stochastic nature of gluon field fluctuations, which reveal themselves at separations of the order of the correlation length λ and lead to the exponential fall-off of the field correlators [see (17)]. It can be shown that if the string acts on the quark with a force σ at large separations, the form factor D should be normalized as

$$D(z^2) = \frac{\sigma}{\pi\lambda^2}\,\exp\left(-\frac{|z|}{\lambda}\right). \tag{36}$$

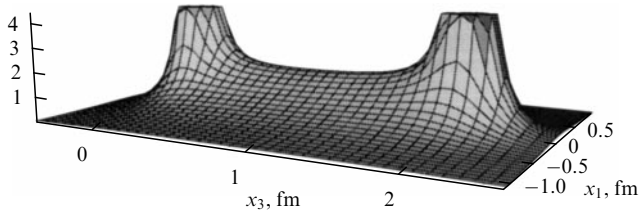

Figure 2. Distribution of the field $\left|\mathcal{E}(x_1, 0, x_3)\right|$ given by Eqn (32) at the quark – antiquark separation 2 fm. The cut peaks of the color-Coulomb field and the string between the quark and the antiquark are clearly distinguished.

Substituting (36) in (32), we calculate the corresponding field

$$\boldsymbol{\mathcal{E}}^D(\mathbf{r}, \mathbf{R}) = \mathbf{n}\,\frac{2\sigma}{\pi}\int_0^{R/\lambda} \mathrm{d}l \left|l\mathbf{n} - \frac{\mathbf{r}}{\lambda}\right| K_1\left(\left|l\mathbf{n} - \frac{\mathbf{r}}{\lambda}\right|\right), \qquad (37)$$

where K_1 is the McDonald function.

The string tension σ can be considered as a scale parameter in QCD. The numerical value $\sigma \approx 0.18$ GeV^2 is determined phenomenologically from the slope of the meson Regge trajectory (see, e.g., Ref. [88]). It is easy to verify that if the point x lies on the symmetry axes, the field $\boldsymbol{\mathcal{E}}^D$ and the nonperturbative part of the static potential corresponding to the form factor D in Eqns (9) and (13) are related as

$$\boldsymbol{\mathcal{E}}^D(\mathbf{r}, \mathbf{R}) = \boldsymbol{\nabla} V^D(r) - \boldsymbol{\nabla} V^D(|\mathbf{r} - \mathbf{R}|)\,. \qquad (38)$$

A relation of this kind can be extracted directly from (20). Indeed, the point x belongs to the minimal surface of the Wilson loop in this case and definitions (20) and (30) coincide because of Gaussian dominance. The distribution of the field $\left|\mathcal{E}(x_1, 0, x_3)\right|$ given by (32) is shown in Fig. 2 at the $\mathrm{Q\bar{Q}}$-separation 2 fm. In the figure, we can see the peaks of the color-Coulomb field (34) over the quark and the antiquark, and the string (37) between them, with the universal profile $\mathcal{E}(\rho)$,

$$\mathcal{E}(\rho) = 2\sigma\left(1 + \frac{\rho}{\lambda}\right)\exp\left(-\frac{\rho}{\lambda}\right), \qquad (39)$$

where ρ is the distance to the $\mathrm{Q\bar{Q}}$ axis.

3.4 Distribution of magnetic currents and Londons' equation

To perform a more detailed analysis of the distribution of magnetic currents (27) in the case of a static quark and antiquark, we apply the first Maxwell equation (25) to the electric field in bilocal approximation (32), (34), and (37). It is then easy to see that the magnetic current $\mathbf{k}$ is given by

$$\mathbf{k} = \mathrm{rot}\,\boldsymbol{\mathcal{E}} \qquad (40)$$

while the magnetic charge is absent. Coulomb field (34) does not contribute to (40) because it is the divergence of a potential.

Nonperturbative field (37) is directed along the quark – antiquark axis, and therefore the magnetic currents are circular, while their magnitude is given by the derivative of field (37) over the transversal coordinate ρ. In the particular case of the saturated string (39), the magnetic field distribution takes the form

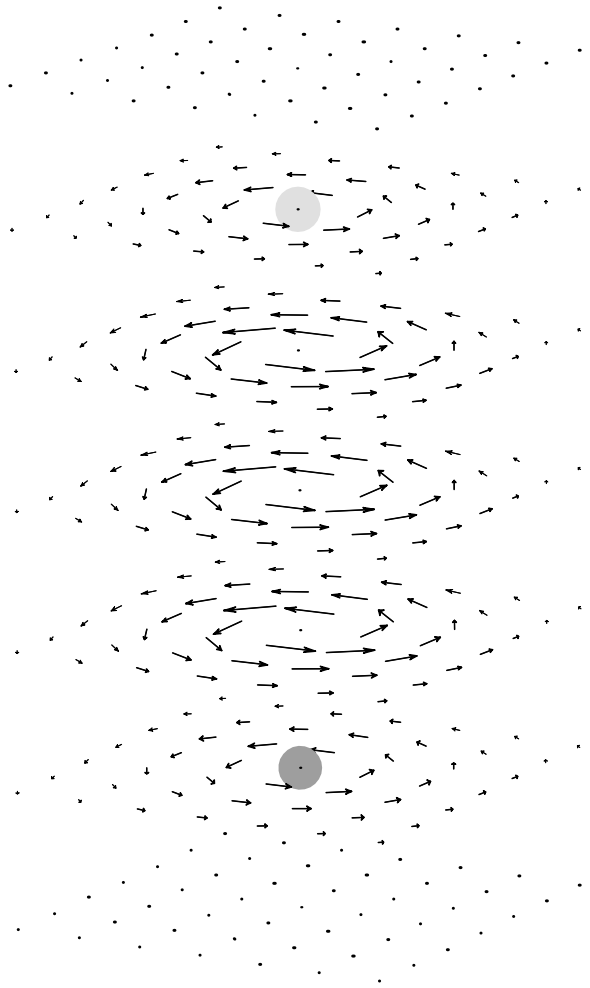

Figure 3. A vector distribution of magnetic currents (37) and (40) at the quark – antiquark separation 2 fm. The positions of the quark and the antiquark are shown by points.

$$k_\varphi(\rho) = -\frac{2\sigma\rho}{\lambda^2}\exp\left(-\frac{\rho}{\lambda}\right), \qquad (41)$$

where k_φ denotes the polar component of the magnetic current in cylindrical coordinates. The vector distribution of magnetic currents is shown in Fig. 3 for the $\mathrm{Q\bar{Q}}$-separation $R = 2$ fm. This distribution resembles that of the electric superconducting currents around the Abrikosov string in superconductors (see Refs [90 – 92] and also textbook [93]).

Moreover, it is easy to see that the 'dual' Londons' equation holds at large distances from the string,

$$\mathrm{rot}\,\mathbf{k} = \lambda^{-2}\boldsymbol{\mathcal{E}} \qquad (42)$$

[the word 'dual' in this context means that the magnetic current stays in the left-hand side of (42) instead of the electric current, while the right-hand side contains the electric field and not the magnetic one]. Indeed, the only component of the polar vector k_φ given by (41) is directed along the z axis and has the form

$$(\mathrm{rot}\,\mathbf{k})_z(\rho) = \frac{1}{\rho}\,\frac{\partial k_\varphi}{\partial \rho} = \gamma(\rho)\,\lambda^{-2}\mathcal{E}(\rho)\,. \qquad (43)$$

The universal profile $\mathcal{E}(\rho)$ is defined by (39), and the function

$$\gamma(\rho) = \frac{-2 + \rho/\lambda}{1 + \rho/\lambda} \tag{44}$$

increases monotonically from -2 and tends to unity as $\gamma(\rho) \approx 1 - 3\lambda/\rho$ for $\rho \gg \lambda$.

We conclude that the confinement mechanism can be explained by the existence of circular magnetic currents (41) that squeeze the electric field into a string and lead to the exponential fall-off outside it [see (39)] and to the dual Meissner equation (43) and (44).

3.5 Vacuum polarization and screening of the coupling constant

We now turn to the Gauss law for the static quark and antiquark,

$$\operatorname{div} \boldsymbol{\mathcal{E}} = \rho\,. \tag{45}$$

The field $\boldsymbol{\mathcal{E}}$ is defined according to (32), (34), and (37),

$$\boldsymbol{\mathcal{E}} = \boldsymbol{\mathcal{E}}^{D_1} + \boldsymbol{\mathcal{E}}^{D}\,. \tag{46}$$

The electric charge density can be written as

$$\rho = 4\pi C_{\mathrm{F}} \alpha_{\mathrm{s}} \bigl(\delta(\mathbf{r}) - \delta(\mathbf{r} - \mathbf{R})\bigr) - \operatorname{div} \boldsymbol{\mathcal{P}}\,. \tag{47}$$

We here introduce the vector $\boldsymbol{\mathcal{P}}$ (as one usually does in continuous media electrodynamics [94]) that takes the non-Abelian interaction of gluon fields at higher orders in the coupling constant into account [see (26)].

We introduce the electric displacement vector field

$$\boldsymbol{\mathcal{D}} = \boldsymbol{\mathcal{E}} + \boldsymbol{\mathcal{P}}\,, \tag{48}$$

and rewrite equation (45) for it as

$$\operatorname{div} \boldsymbol{\mathcal{D}} = 4\pi C_{\mathrm{F}} \alpha_{\mathrm{s}} \bigl(\delta(\mathbf{r}) - \delta(\mathbf{r} - \mathbf{R})\bigr)\,. \tag{49}$$

Because the right-hand side of (49) involves the divergence of Coulomb field (34), assuming perturbative dominance of the function D_1 [see (35)], we obtain the relation

$$\operatorname{div} \boldsymbol{\mathcal{P}} = -\operatorname{div} \boldsymbol{\mathcal{E}}^{D}\,. \tag{50}$$

According to (37),

$$\operatorname{div} \boldsymbol{\mathcal{E}}^{D} = \tilde{\rho}(r) - \tilde{\rho}(|\mathbf{r} - \mathbf{R}|)\,, \tag{51}$$

$$\tilde{\rho}(r) = \frac{2\sigma}{\pi\lambda^2}\, r\, K_1\left(\frac{r}{\lambda}\right). \tag{52}$$

This means that the polarization vector can be represented as a difference of two central vectors,

$$\boldsymbol{\mathcal{P}}(\mathbf{r}, \mathbf{R}) = \tilde{P}(r)\, \frac{\mathbf{r}}{r} - \tilde{P}(|\mathbf{r} - \mathbf{R}|)\, \frac{\mathbf{r} - \mathbf{R}}{|\mathbf{r} - \mathbf{R}|}\,, \tag{53}$$

satisfying the equation

$$\frac{1}{r^2}\, \frac{\partial}{\partial r}\, r^2 \tilde{P}(r) = -\tilde{\rho}(r)\,. \tag{54}$$

It follows from (54) that

$$\tilde{P}(r) = -\frac{\tilde{Q}(r)}{r^2}\,, \qquad \tilde{Q}(r) = \frac{2\sigma\lambda^2}{\pi} \int_0^{r/\lambda} \mathrm{d}x\, x^3 K_1(x)\,, \tag{55}$$

where $\tilde{Q}$ is the screening charge. Because of confinement, the field must fall off faster than any power at large distances from the quark and antiquark, and therefore the full charge

$$Q(r) \equiv C_{\mathrm{F}} \alpha_{\mathrm{s}}(r) - \tilde{Q}(r) \tag{56}$$

vanishes. In particular, this implies the relation [40]

$$C_{\mathrm{F}} \alpha_{\mathrm{s}} = 3\sigma\lambda^2 \tag{57}$$

between the frozen strong coupling [99, 100] and the key parameters responsible for confinement. Inserting $\alpha_{\mathrm{s}} = 0.42$ [99, 100, 95, 96] in (57), we obtain $\lambda = 0.2$ fm.

The behavior of the charge $Q(r)$ at the standard value $\alpha_{\mathrm{s}} = 0.42$ is shown in Fig. 4. It follows from Fig. 5, where the running coupling pattern is shown by the dotted curve, that this approximation is valid at $r \gtrsim 0.4$ fm. (The definition of the running coupling and corresponding formulas can be found in Refs [95, 96].) The behavior of the running charge $Q^{\mathrm{run}}(r)$ is shown by the solid curve. As can be seen from the figure, the effective charge has a maximum at $r \approx 0.3$ fm.

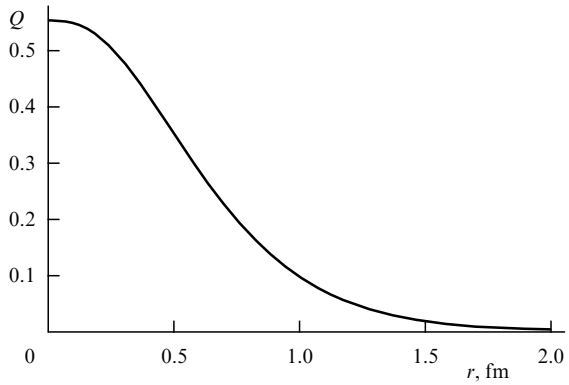

Figure 4. The effective charge $Q(r)$ given by (56) vs. the distance from the quark for $\sigma = 0.18$ GeV^2, $\lambda = 0.2$ fm, and the constant value $\alpha_{\mathrm{s}} = 0.42$.

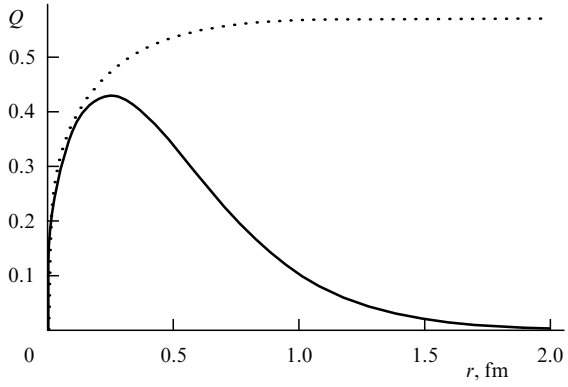

Figure 5. The running background coupling $C_{\mathrm{F}}\alpha_{\mathrm{s}}(r)$ [95, 96] (dotted curve) and the running effective charge $Q^{\mathrm{run}} = C_{\mathrm{F}}\alpha_{\mathrm{s}}(r) - \tilde{Q}(r)$ (solid curve) vs. the distance from the quark.

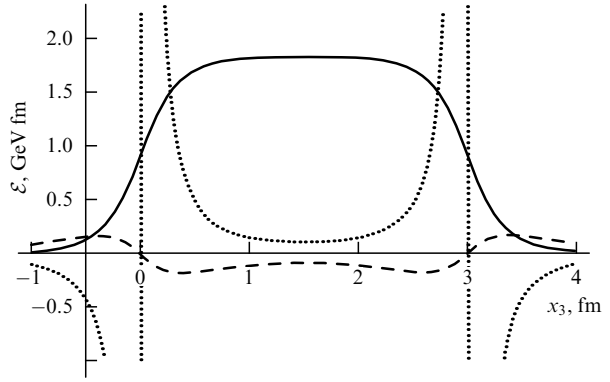

Figure 6. Distributions of the projections of the fields $\boldsymbol{\mathcal{E}}^D(0,0,x_3)$ (solid curve), $\boldsymbol{\mathcal{P}}(0,0,x_3)$ (dashed curve), and $\boldsymbol{\mathcal{E}}^{\rm c}(0,0,x_3)$ (dotted curve) on the quark – antiquark axis at the $\mathrm{Q\bar{Q}}$ separation 3 fm.

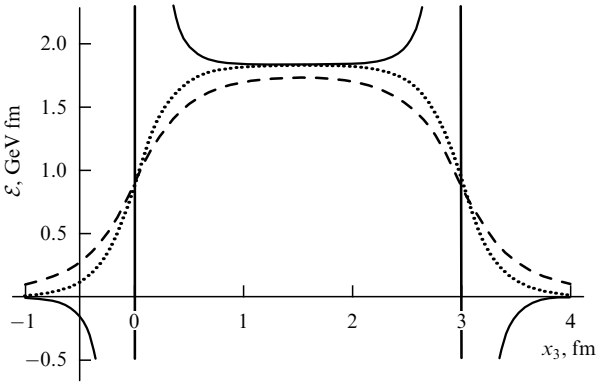

Figure 7. Distributions of the projections of the fields $\boldsymbol{\mathcal{E}}^D(0,0,x_3)$ (dotted curve), $\boldsymbol{\mathcal{E}}^D(0,0,x_3)+\boldsymbol{\mathcal{P}}(0,0,x_3)$ (dashed curve), and $\boldsymbol{\mathcal{D}}(0,0,x_3)$ (solid curve) on the quark – antiquark axis at the $\mathrm{Q\bar{Q}}$ separation 3 fm.

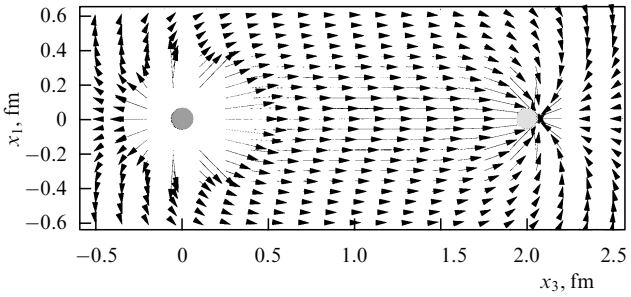

Figure 8. Vector distribution of the field $\boldsymbol{\mathcal{D}}(x_1,0,x_3)$. Positions of the quark and the antiquark are marked by points.

We now turn to the figures characterizing dielectric properties of the vacuum. In Fig. 6, the projections of the fields $\boldsymbol{\mathcal{E}}^D(0,0,x_3)$, $\boldsymbol{\mathcal{P}}(0,0,x_3)$, and $\boldsymbol{\mathcal{E}}^{\rm c}(0,0,x_3)$ on the quark – antiquark axis are shown (the distance between the quark and the antiquark is 3 fm). We note that the fields $\boldsymbol{\mathcal{P}}$ and $\boldsymbol{\mathcal{E}}^{\rm c}$ exactly cancel in the middle of the string. This can also be seen from Fig. 7, where the projections of fields $\boldsymbol{\mathcal{E}}^D(0,0,x_3)$, $\boldsymbol{\mathcal{E}}^D(0,0,x_3)+\boldsymbol{\mathcal{P}}(0,0,x_3)$, and $\boldsymbol{\mathcal{D}}(0,0,x_3)$ on the quark – antiquark axis are plotted. In Fig. 8, the vector distribution of the displacement field $\boldsymbol{\mathcal{D}}(x_1,0,x_3)$ is shown, demonstrating that the field is squeezed into a tube with a width of the order of $\lambda = 0.2$ fm. In Fig. 9, the vector distribution of the solenoidal field $\boldsymbol{\mathcal{E}}^D(x_1,0,x_3)+\boldsymbol{\mathcal{P}}(x_1,0,x_3)$ is plotted.

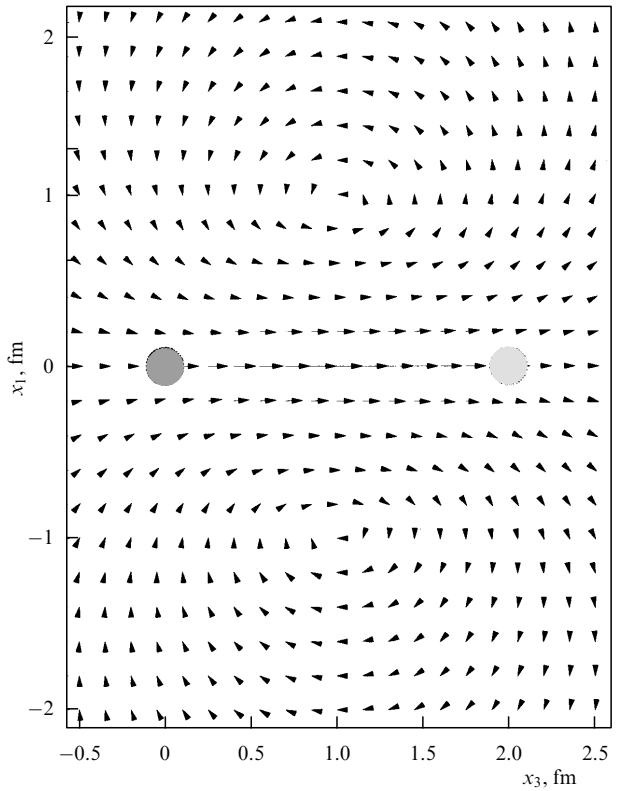

Figure 9. Vector distribution of the solenoid field $\boldsymbol{\mathcal{E}}^D(x_1,0,x_3)+\boldsymbol{\mathcal{P}}(x_1,0,x_3)$. Positions of the quark and the antiquark are marked by points.

We define the isotropic dielectric function $\varkappa(r)$ as

$$\boldsymbol{\mathcal{P}} = \varkappa \boldsymbol{\mathcal{E}}^{\rm c} \tag{58}$$

and the dielectric permittivity as $\varepsilon = 1 + \varkappa$. We then obtain

$$\varkappa(r) = -\frac{\tilde{Q}(r)}{C_{\rm F}\alpha_{\rm s}(r)}\,, \tag{59}$$

$$\varepsilon(r) = \frac{Q(r)}{C_{\rm F}\alpha_{\rm s}(r)}\,. \tag{60}$$

In particular, at large distances ($r \gg \lambda$), the vacuum dielectric permittivity is exponentially small,

$$\varepsilon(r)\big|_{r\to\infty} = \frac{1}{3(2\pi)^{3/2}}\left(\frac{r}{\lambda}\right)^{-5/2}\exp\left(-\frac{r}{\lambda}\right). \tag{61}$$

This smallness of dielectric permittivity (61) means that the color-Coulomb field is absent at a large enough distance from sources outside the string as well as on it.

4. Hadrons with three static sources

4.1 Green's functions and Wilson loops

We now consider hadrons with three static color sources: baryons and three gluon glueballs. Because hadrons are nonlocal extended objects, we use the nonlocal quark and gluon operators

$$q^{\alpha}(x,Y) \equiv q^{\beta}(x)\,\Phi^{\alpha}_{\beta}(x,Y)\,, \tag{62}$$

$$g_a(x,Y) \equiv g_b(x)\,\Phi_{ab}(x,Y)\,, \tag{63}$$

and also the local gluon operator

$$G_\alpha^\beta(x) \equiv g_a(x)\, t_\alpha^{(a)\beta}\,.$$

Here, g_a denotes the valence gluon operator of the background perturbation theory [99, 100]. We note that $G_\alpha^\beta(x)$ transforms as $G_\alpha^\beta \to U_{\beta'}^{+\beta} G_{\alpha'}^{\beta'} U_\alpha^{\alpha'}$ under gauge transformations.

Gauge invariant combinations of these operators can be constructed using symmetric tensors δ_α^β, δ^{ab}, and d^{abc} and antisymmetric ones $e_{\alpha\beta\gamma}$ and f^{abc},

$$B_{\rm Y}(x,y,z,Y) = e_{\alpha\beta\gamma}\, q^\alpha(x,Y)\, q^\beta(y,Y)\, q^\gamma(z,Y)\,, \tag{64}$$

$$G_{\rm Y}^{(f)}(x,y,z,Y) = f^{abc} g_a(x,Y)\, g_b(y,Y)\, g_c(z,Y)\,, \tag{65}$$

$$G_{\rm Y}^{(d)}(x,y,z,Y) = d^{abc} g_a(x,Y)\, g_b(y,Y)\, g_c(z,Y)\,, \tag{66}$$

$$G_\Delta(x,y,z) = G_\alpha^\beta(x)\, \Phi_\beta^\gamma(x,y)\, G_\gamma^\delta(y)\, \Phi_\delta^\varepsilon(y,z)\, G_\varepsilon^\rho(z)\, \Phi_\rho^\alpha(z,x)\,. \tag{67}$$

The first three constructions have a Y-type structure with the string junction at the point Y where the color indices are contracted with the (anti-) symmetric tensor, and the latter has a Δ-type structure. We stress that the Δ-type wave function is possible only for glueballs but not for baryons [98].

The hadron Green's function has the form

$$\mathcal{G}_i(\bar X, X) = \left\langle \Psi_i^+(\bar X)\, \Psi_i(X) \right\rangle, \tag{68}$$

where $\Psi_i = G_\Delta, G_{\rm Y}, B_{\rm Y}$ and $X = x, y, z$ in the case of G_Δ and x, y, z, Y for Y-states. The vacuum average $\langle \ldots \rangle$ leads to the product of Green's functions of quarks or valence gluons for hadrons with the static sources, which are proportional to the phase factors

$$\begin{aligned} &\left\langle \bar q_\beta(\bar x)\, q^\alpha(x) \right\rangle \propto \Phi_\beta^\alpha(\bar x, x)\,, \\ &\left\langle g_a(\bar x)\, g_b(x) \right\rangle \propto \Phi_{ab}(\bar x, x)\,. \end{aligned} \tag{69}$$

(The same formulas hold for relativistic sources if the Fock–Feynman–Schwinger representation is used [9, 10, 101–103].) Therefore, as discussed in Section 2, the hadron Green's function is proportional to the gauge-invariant combination called the Wilson loop of this hadron.

Baryons and glueballs of the Y-type are characterized by the Wilson loops

$$\mathcal{W}_{\rm B} = \frac{1}{6} \left\langle \epsilon_{\alpha\beta\gamma} \epsilon^{\alpha'\beta'\gamma'}\, \Phi_{\alpha'}^\alpha(C_1)\, \Phi_{\beta'}^\beta(C_2)\, \Phi_{\gamma'}^\gamma(C_3) \right\rangle, \tag{70}$$

$$\mathcal{W}_{\rm G}^{{\rm Y},f} = \frac{1}{24} \left\langle f^{abc} f^{a'b'c'}\, \Phi^{aa'}(C_1)\, \Phi^{bb'}(C_2)\, \Phi^{cc'}(C_3) \right\rangle, \tag{71}$$

$$\mathcal{W}_{\rm G}^{{\rm Y},d} = \frac{3}{40} \left\langle d^{abc} d^{a'b'c'}\, \Phi^{aa'}(C_1)\, \Phi^{bb'}(C_2)\, \Phi^{cc'}(C_3) \right\rangle. \tag{72}$$

Trajectories C_i formed by the sources are shown in Fig. 10. An expression for the Wilson loop of a Δ-type glueball can be found in Ref. [87]. In the confinement phase, it can be approximated as the product of three meson Wilson loops,

$$\mathcal{W}_{\rm G}^\Delta(X, \bar X) = W(\bar x, \bar y | x, y)\, W(\bar y, \bar z | y, z)\, W(\bar z, \bar x | z, x)\,. \tag{73}$$

The corresponding contours are shown in Fig. 11.

4.2 Static potentials

Static potentials of hadrons with three static sources are calculated in the bilocal approximation of the field correlator

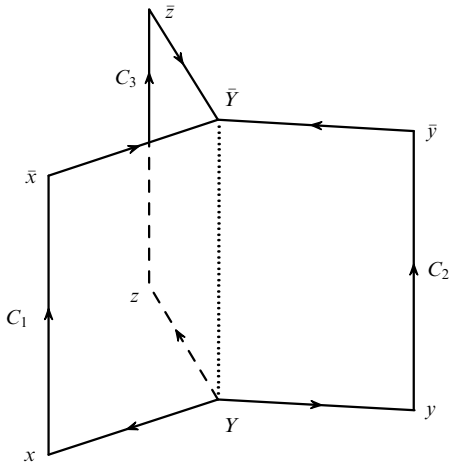

Figure 10. A W-loop of the Y-type.

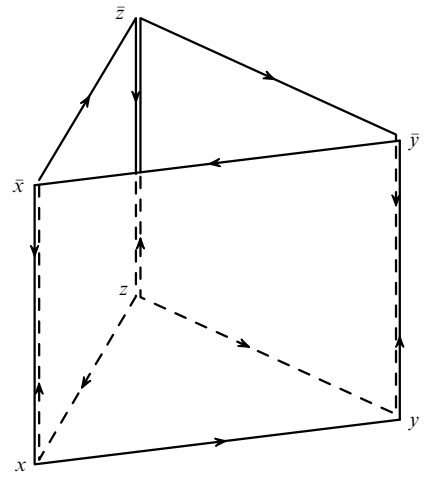

Figure 11. A W-loop of the Δ-type.

method [98, 104] in the same way as the meson ones. For hadrons of the Y-type, we let $\mathbf{n}^{(a)}$ denote the unit vector directed from the string junction to the ath quark and R_a the separation between this quark and the string junction. Then the potential in the baryon is given by

$$V_{\rm B}(R_1, R_2, R_3) = \left(\sum_{a=b} - \sum_{a<b} \right) n_i^{(a)} n_j^{(b)} \times \int_0^{R_a} \int_0^{R_b} {\rm d}l\, {\rm d}l' \int_0^\infty {\rm d}t\, \mathcal{D}_{i4,j4}(z_{ab})\,, \tag{74}$$

where $z_{ab} = (l\mathbf{n}^{(a)} - l'\mathbf{n}^{(b)}, t)$.

We can represent potential (74) in the form

$$V_{\rm B} = V^{\rm c} + V^{\rm d} + V^{\rm nd}\,, \tag{75}$$

where

$$V^{\rm c} = -\frac{C_{\rm F}\alpha_{\rm s}}{2} \sum_{i<j} \frac{1}{r_{ij}} \tag{76}$$

is the one-gluon exchange potential and r_{ij} is the distance between the ith and the jth quark. We take the charge screening into account by replacing $C_{\rm F}\alpha_{\rm s}$ in (76) with Q defined in (56). The terms $V^{\rm d}$ and $V^{\rm nd}$ in (75) denote the diagonal and nondiagonal parts of the potential correspond-

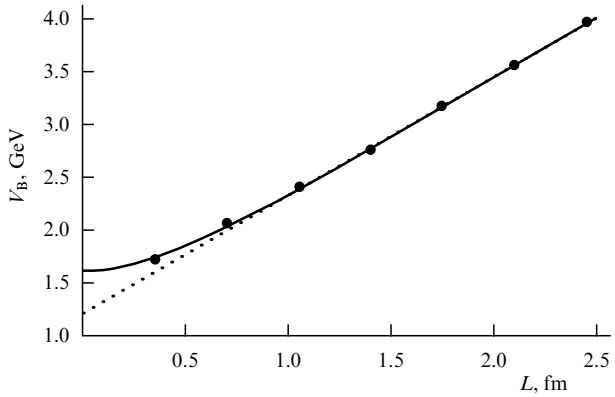

Figure 12. Potential (74) in the baryon with the color-Coulomb part contracted (solid curve), in comparison with the lattice data [105] (points) depending on the total length of the baryon string L. The value of the string tension is $\sigma = 0.22$ GeV^2. According to (57), the corresponding value of the correlation length is $\lambda = 0.18$ fm.

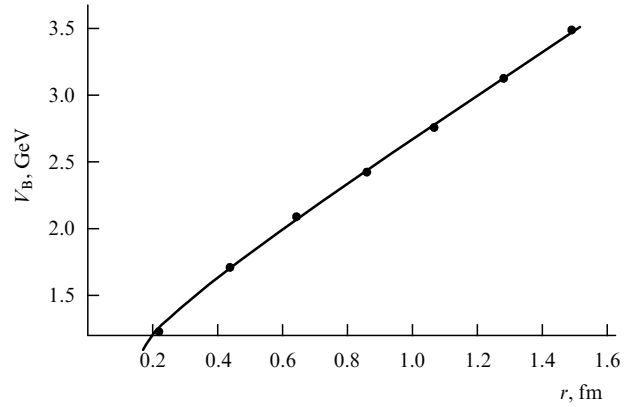

Figure 13. The dependence of the baryon potential in an equilateral triangle on the quark separation r (solid curve) in comparison with the lattice data [106] (points). The value of the string tension is $\sigma = 0.17$ GeV^2 ($\lambda = 0.21$ fm).

ing to the correlator D [$V^{\rm d}$ is determined by the first and $V^{\rm nd}$ by the second sum in (74)]. Explicit expressions for $V^{\rm d}$ and $V^{\rm nd}$ can be found in Ref. [104]. We just note here that $V^{\rm d}$ is a sum of the quark–antiquark potentials V^D in (9) and (13),

$$V^{\rm d}(R_1, R_2, R_3) = \sum_a V^D(R_a)\,. \tag{77}$$

A typical feature of potential (74) is an increase in its slope with the distance between sources. The baryon potential with the color-Coulomb part subtracted is shown in Fig. 12 in comparison with the lattice data [105] as a function of the total length $L = \sum_a R_a$ of the baryon string. A tangent with the slope σ is shown by a dotted line. We can see from the figure that the potential slope becomes significantly less than σ at $L \lesssim 1$ fm. This effect is induced by the influence of the correlation length of the confining fields [104]. The dependence of the baryon potential in an equilateral triangle on the quark separation is given in Fig. 13 in comparison with the lattice data [106]. We note the agreement between analytic and lattice calculations with an accuracy within a few dozen MeV.

For the Y-glueball potential, the relation

$$\frac{V_{\rm G}^{\rm Y}}{V_{\rm B}} = \frac{C_8}{C_3} \tag{78}$$

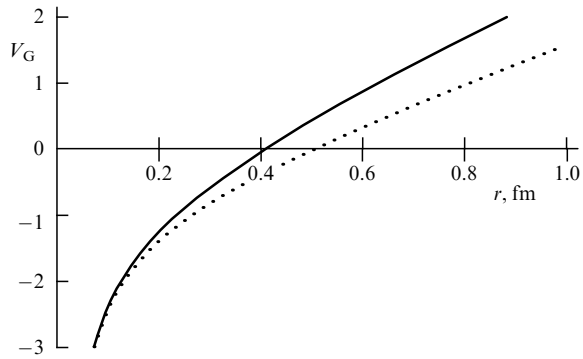

Figure 14. Potentials of the three-gluon glueballs $V_{\rm G}^{\rm Y}$ (solid curve) and $V_{\rm G}^{\Delta}$ (dotted curve) in an equilateral triangle depending on the separation r between the sources.

holds, where $C_3 = (N_{\rm c}^2 - 1)/2N_{\rm c}$ and $C_8 = N_{\rm c}$ are the quadratic Casimir operators in the fundamental and adjoint representations. It is seen from (78) that hadrons with a Y string demonstrate Casimir scaling.

The Δ-glueball potential in the case of an equilateral triangle with a side r has the form [98]

$$V_{\rm G}^{\Delta}(r) = \frac{C_8}{C_3}\, V^{\rm c}(r) + V^{\rm d}(r) - 2V^{\rm nd}(r)\,. \tag{79}$$

We note that $V^{\rm d}$ and $V^{\rm nd}$ depend on the valence gluon separation but not on the separation between the gluon and the center of the triangle, and that the term $-2V^{\rm nd}$ corresponds to the interaction of three effective quark–antiquark Wilson loops. The potentials $V_{\rm G}^{\rm Y}$ and $V_{\rm G}^{\Delta}$ in the equilateral triangle are shown in Fig. 14 as functions of the source separation r. The potential $V_{\rm G}^{\rm Y}$ goes above $V_{\rm G}^{\Delta}$ because of the positive contribution of the nondiagonal term $V^{\rm nd}$ to the Y-type glueball and the negative contribution to the triangular one, and also because of the greater slope of the diagonal term $V^{\rm d}$ in the case of the Y-glueball. The main energy gain comes from the attraction of the effective quark–antiquark Wilson loops in (79).

4.3 Field distributions

The effective field distributions in baryons and glueballs are given in Ref. [40]. The baryon field is defined there as the square average

$$(\boldsymbol{\mathcal{E}}^{(\rm B)})^2 = \frac{2}{3}\left((\boldsymbol{\mathcal{E}}_{(1)}^{\rm B})^2 + (\boldsymbol{\mathcal{E}}_{(2)}^{\rm B})^2 + (\boldsymbol{\mathcal{E}}_{(3)}^{\rm B})^2\right) \tag{80}$$

of the fields $\boldsymbol{\mathcal{E}}_{(i)}^{\rm B}$ calculated for the probe plaquette attached to the trajectory C_i,

$$\boldsymbol{\mathcal{E}}_{(1)}^{\rm B}(\mathbf{x}, \mathbf{R}^{(1)}, \mathbf{R}^{(2)}, \mathbf{R}^{(3)}) = \boldsymbol{\mathcal{E}}^{\rm M}(\mathbf{x}, \mathbf{R}^{(1)}) - \frac{1}{2}\,\boldsymbol{\mathcal{E}}^{\rm M}(\mathbf{x}, \mathbf{R}^{(2)}) - \frac{1}{2}\,\boldsymbol{\mathcal{E}}^{\rm M}(\mathbf{x}, \mathbf{R}^{(3)})\,. \tag{81}$$

The coefficient 2/3 in (80) is chosen such that the field acting on each quark is equal to σ.

According to (80) and (81), the field in the baryon is expressed through the fields of effective quark–antiquark pairs, with the positions of the antiquarks coinciding with the string junction. The distribution of the field $\boldsymbol{\mathcal{E}}^{(\rm B)}$, with only the contribution of the form factor D taken into account, is shown in Figs 15 and 16 in the plane of quarks forming an equilateral triangle with sides 1 and 3.5 fm, respectively. In Fig. 16, one can see three plateaus with a saturated profile and

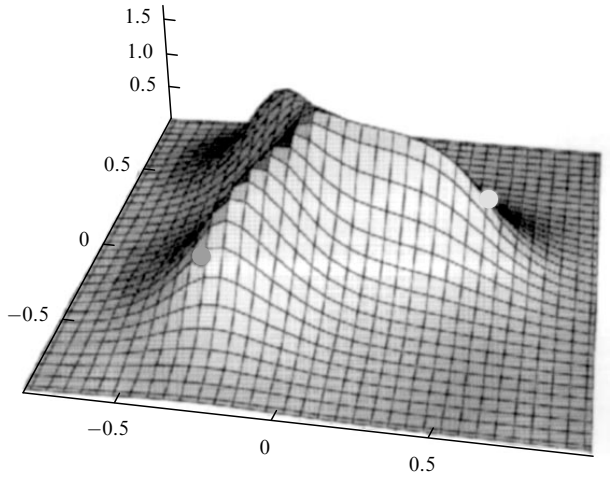

Figure 15. Distribution of the field $\mathcal{E}^{(\mathrm{B})}$ given by (80) and (81) in GeV/fm with only the correlator D contribution considered in the quark plane for an equilateral triangle with the side 1 fm. Coordinates are given in fm, positions of the quarks are marked by points.

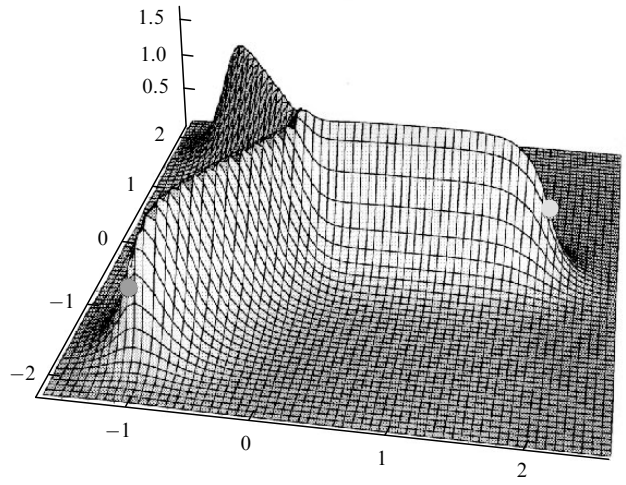

Figure 16. Distribution of the field $\mathcal{E}^{(\mathrm{B})}$ given by (80) and (81) in GeV/fm with only the correlator D contribution considered in the quark plane for an equilateral triangle with the side 3.5 fm. Coordinates are given in fm, positions of the quarks are marked by points.

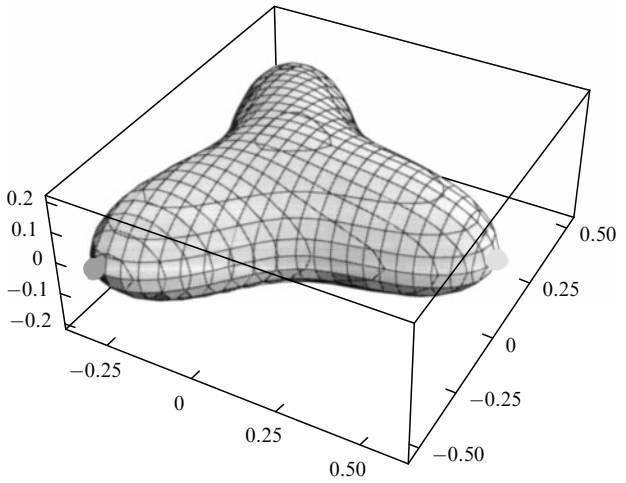

Figure 17. The surface $|\mathcal{E}^{(\mathrm{B})}(\mathbf{x})| = \sigma$ at the quark separations 1 fm. Coordinates are given in fm, positions of the quarks are marked by points.

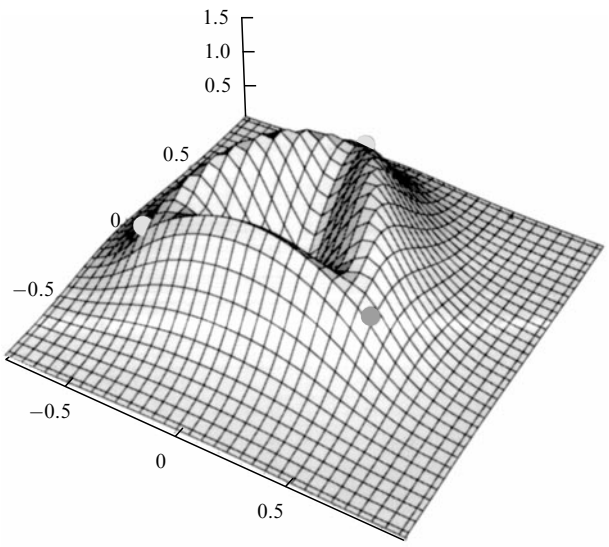

Figure 18. Distribution of the field $|\mathcal{E}_{\Delta}^{(\mathrm{G})}(\mathbf{x})|$ given by (82) in GeV/fm of the triangular glueball in the plane of valence gluons with the separations 1 fm. Coordinates are given in fm, positions of the valence gluons are marked by points.

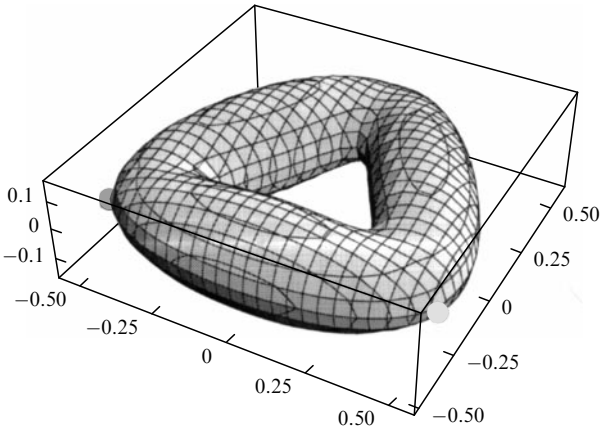

Figure 19. The surface $|\mathcal{E}_{\Delta}^{(\mathrm{G})}(\mathbf{x})| = \sigma$ at the valence gluon separations 1 fm. Coordinates are given in fm, positions of the valence gluons are marked by points.

small growth of the field around the string junction point, with the relative difference of values amounting to 1/16. A surface formed by the confining field with the value σ is shown in Fig. 17 for the quark separations 1 fm. One can see small convexity in the region of the string junction.

The field in the Δ-type glueball is a sum of meson fields with gluon pairs acting as the effective sources [40],

$$\mathcal{E}_{\Delta}^{(\mathrm{G})}(\mathbf{x},\mathbf{r}^{(1)},\mathbf{r}^{(2)},\mathbf{r}^{(3)}) = \sum_{i=1}^{3}\mathcal{E}^{\mathrm{M}}(\mathbf{x}-\mathbf{r}^{(i)},\mathbf{r}^{(i+1)\bmod 3}-\mathbf{r}^{(i)}), \tag{82}$$

where $\mathbf{r}^{(i)}$ denotes the position of the ith valence gluon. The field distribution $|\mathcal{E}_{\Delta}^{(\mathrm{G})}(\mathbf{x})|$ in the valence gluon plane is shown in Fig. 18 at the gluon separations 1 fm. In Fig. 19, the surface $|\mathcal{E}_{\Delta}^{(\mathrm{G})}(\mathbf{x})| = \sigma$ is plotted for the same gluon separations.

We note that according to (38), the static quark–antiquark potential can be calculated as the work of the confining force acting on a quark to move it to a distance R

from the antiquark. The analogous relation is valid for the field and potential of Δ-type glueball (79) and (82). The nondiagonal part of the Δ-glueball potential $V^{\rm nd}$ is then equal to the work of the force acting on the given (effective) quark from the external string, and is therefore related to the interference (superposition) of the meson fields $\mathcal{E}^{\rm M}$ in the neighborhood of valence gluons of the order of λ.

5. Conclusions

In this paper, we have systematically treated the vacuum fields in QCD, the confinement mechanism, the QCD string formation, and, finally, the field distribution inside hadrons.

Everywhere we have used the field correlators as a universal gauge-invariant formalism that allows describing all phenomena encountered in QCD. In the description of vacuum fields, the most important property is the Gaussian dominance: the lowest (Gaussian) correlator is dominating on the minimal area surface of the Wilson loop, and there are sufficient grounds for the statement that the total distribution of higher correlators does not exceed a few percent. This phenomenon, found on the lattice [68], is not yet fully understood (see also Refs [11, 16] in this respect), although it gives an explicit dynamic picture, which is possibly incompatible with the old physics of the instanton gas, of Z_2-fluxes, etc.

Therefore, we can assert that the picture of the maximally stochastic QCD vacuum is a very good approximation of reality. We recall that the measure of coherence is associated with the weight of the contribution of higher correlators; for example, the total contribution of higher (non-Gaussian) correlators is dominant for the instanton gas. Moreover, the vacuum correlation length λ (i.e., a factor in the exponent for asymptotics of the Gaussian correlator) is relatively small, $\lambda \sim 0.2$ fm for the quenched vacuum. This value is much smaller than the typical hadron radius, ~ 1 fm. Theoretically, the smallness of λ is connected to a large mass gap for glueballs and gluelumps [12 – 14].

We now turn to the confinement mechanism. From the standpoint of field correlators, confinement occurs due to a specific term in the Gaussian correlator, denoted $D(x^2)$, which violates Bianchi identities in the Abelian case and is therefore absent in the case of QED. If, however, one considers compact U(1) theory with magnetic monopoles present in the vacuum, then the function $D(x^2)$ is nonzero; it is proportional to the monopole currents correlator. The next step is to find the source of $D(x^2)$ (i.e., the source of confinement) in the non-Abelian theory. This was done in Ref. [7], where the derivatives of $D(x^2)$ were connected to the triple correlator $\langle EEB \rangle$.

Thus, the problem of establishing the confinement mechanism in the formalism of field correlators reduces to the problem of calculating $D(x^2)$ and the triple correlator and of finding the conditions for its appearance (disappearance) in QCD, for example, as functions of temperature or baryon density. Lattice calculations confirm the disappearance of $D(x^2)$ at the deconfinement temperature $T_{\rm c}$, and consequently the confinement picture in the framework of the present method is confirmed. We expect that at the next step (by computing correlators [including $D(x^2)$] with the help of the gluelump Green's functions in the whole x region), the method of field correlators will be made self-consistent, and the problem of confinement will be solved quantitatively and as a matter of principle.

At the same time, this universal formalism of field correlators can be used to study the distribution of effective fields and currents defined via the Wilson loop. This representation (see Section 3), on the one hand, enables one to describe the dual Meissner effect [18, 19], and on the other hand, it keeps contact with the effective Lagrangian approach of Adler and Piran [25] and dielectric vacuum models ([27, 28] and subsequent papers). Indeed, the field correlator method not only allows this approximate qualitative interpretation, but also yields explicit expressions for the density of effective electric charges and effective magnetic currents. Given by the gradient of the color-Coulomb potential at small distances, the effective field condenses into a tube on the characteristic hadron scale and ensures confinement. Correspondingly, the strong coupling constant is screened due to vacuum polarization by non-Abelian gluon interactions.

Finally, we summarize the contents of Section 4, devoted to field distributions inside hadrons with three constituents. Here the field correlator method is the only quantitative analytic method, and its comparison with numerical (lattice) results is very interesting. We note that we here deal with only two parameters — the string tension σ and the correlation length λ, with λ expressed through σ and σ playing the role of the scale parameter related to $\Lambda_{\rm QCD}$. The baryon potential computed in this way [98] is in good agreement with lattice calculations and gives an independent confirmation that baryon strings have the Y-type structure with the string junction.

Moreover, the field correlator method explains the smaller slope of the baryon potential at the typical hadron distances known from the baryon phenomenology: the decrease of the slope is caused by the string interference effects related to a nonzero correlation length λ. The three-gluon glueballs, in contrast to baryons, can have the structure of both Y-type and Δ-type [98]. However, the latter is preferred energetically. In the concluding part of Section 4, the field distributions in baryons and in the Δ-type glueballs are given, where one can visualize the shape of the string in these hadrons.

Summarizing, we can say that the universal language of the field correlator method turns out to be extremely convenient in all cases considered. In particular, it enables one to formulate the gauge-invariant description of the QCD vacuum as some medium whose properties provide confinement.

The authors are grateful to L B Okun' for his support and interest and to N O Agasyan, D V Antonov, and M I Polikarpov for numerous discussions.

This work was supported by the grant INTAS 00-110 and INTAS 00-00366 (D K and Yu S). V Sh is grateful to FOM and Dutch National Scientific Fund (NOW), Netherlands for financial support.

References

1. Slavnov A A, Faddeev L D *Vvedenie v Kvantovuyu Teoriyu Kalibrovochnykh Poleĭ* (Gauge Fields: an Introduction to Quantum Theory) (Moscow: Nauka, 1978) [Translated into English (Redwood, CA: Addison-Wesley, 1991)]
2. Ynduráin F J *Quantum Chromodynamics: an Introduction to the Theory of Quarks and Gluons* (New York: Springer-Verlag, 1983)
3. Shifman M A, Vainshtein A I, Zakharov V I *Nucl. Phys. B* **147** 385, 448 (1979)
4. Simonov Yu A *Usp. Fiz. Nauk* **166** 337 (1996) [*Phys. Usp.* **39** 313 (1996)]

5. Dosch H G *Phys. Lett. B* **190** 177 (1987)
6. Dosch H G, Simonov Yu A *Phys. Lett. B* **205** 339 (1988)
7. Simonov Yu A *Nucl. Phys. B* **307** 512 (1988)
8. Di Giacomo A et al. *Phys. Rep.* **372** 319 (2002)
9. Simonov Yu A, Tjon J A *Ann. Phys.* (New York) **228** 1 (1993)
10. Simonov Yu A, Tjon J A *Ann. Phys.* (New York) **300** 54 (2002)
11. Shevchenko V I, Simonov Yu A *Int. J. Mod. Phys. A* **18** 127 (2003)
12. Foster M, Michael C (UKQCD Collab.) *Nucl. Phys. B*: *Proc. Suppl.* **63** 724 (1998)
13. Foster M, Michael C (UKQCD Collab.) *Phys. Rev. D* **59** 094509 (1999)
14. Simonov Yu A *Nucl. Phys. B* **592** 350 (2001)
15. Simonov Yu A, hep-ph/9712250
16. Shevchenko V I *Phys. Lett. B* **550** 85 (2002)
17. Simonov Yu A, hep-ph/0211330
18. 't Hooft G, in *High Energy Physics*: *Proc. of the EPS Intern. Conf., Palermo, Italy, 23–28 June 1975* (Intern. Physics Series, 6, Ed. A Zichichi) (Bologna: Compositori, 1976)
19. Mandelstam S *Phys. Lett. B* **53** 476 (1975)
20. Di Giacomo A, hep-lat/0204032
21. Di Giacomo A *Nucl. Phys. A* **702** 73 (2002)
22. Suzuki T et al. *Nucl. Phys. B*: *Proc. Suppl.* **106–107** 631 (2002)
23. Chernodub M N et al., hep-lat/0103033
24. Bornyakov V G et al., hep-lat/0210047
25. Adler S L, Piran T *Phys. Lett. B* **113** 405 (1982)
26. Adler S L, Piran T *Rev. Mod. Phys.* **56** 1 (1984)
27. Friedberg R, Lee T D *Phys. Rev. D* **15** 1694 (1977)
28. Friedberg R, Lee T D *Phys. Rev. D* **16** 1096 (1977)
29. Agasyan N O, Voskresensky D N *Phys. Lett. B* **127** 448 (1983)
30. Migdal A B, Agasyan N O, Khokhlachev S B *Pis'ma Zh. Eksp. Teor. Fiz.* **41** 405 (1985) [*JETP Lett.* **41** 497 (1985)]
31. Schuh A, Pirner H-J, Wilets L *Phys. Lett. B* **174** 10 (1986)
32. Pirner H-J *Prog. Part. Nucl. Phys.* **29** 33 (1992)
33. Traxler C T, Mosel U, Biró T S *Phys. Rev. C* **59** 1620 (1999)
34. Martens G et al., hep-ph/0303017
35. Makeenko Yu M, Migdal A A *Yad. Fiz.* **32** 838 (1980) [*Sov. J. Nucl. Phys.* **32** 431 (1980)]
36. Polyakov A M *Gauge Fields and Strings* (Chur: Harwood Acad. Publ., 1987) [Translated into Russian (Moscow: ITF im. L D Landau, 1995)]
37. Del Debbio L, Di Giacomo A, Simonov Yu A *Phys. Lett. B* **332** 111 (1994)
38. Kuzmenko D S, Simonov Yu A *Phys. Lett. B* **494** 81 (2000)
39. Kuzmenko D S, Simonov Yu A *Yad. Fiz.* **64** 110 (2001) [*Phys. Atom. Nucl.* **64** 107 (2001)]
40. Kuzmenko D S, Simonov Yu A, in *NPD-2002 Conf., ITEP, Moscow, Dec. 2–6, 2002*; hep-ph/0302071
41. Ichie H et al., ITEP-LAT/2002-24; KANAZAWA 02-33; hep-lat/0212024
42. Bornyakov V G et al. *Usp. Fiz. Nauk* **174** 19 (2004) [*Phys. Usp.* **47** 000 (2004)]
43. Bali G S *Phys. Rep.* **343** 1 (2001)
44. 't Hooft G *Nucl. Phys. B* **72** 461 (1974)
45. Wegner F *J. Math. Phys.* **12** 2259 (1971)
46. Wilson K G *Phys. Rev. D* **10** 2445 (1974)
47. Volterra V, Hostinský B *Opérations Infinitésimales Linéaires*; *Applications aux Équations Différentielles et Fonctionnelles* (Paris: Gauthiers-Villars, 1938)
48. Halpern M B *Phys. Rev. D* **19** 517 (1979)
49. Bralic N E *Phys. Rev. D* **22** 3090 (1980)
50. Arefeva I Ya *Teor. Mat. Fiz.* **43** 111 (1980) [*Theor. Math. Phys.* **43** 353 (1980)]
51. Simonov Yu A *Yad. Fiz.* **50** 213 (1989) [*Sov. J. Nucl. Phys.* **50** 134 (1989)]
52. Hirayama M, Ueno M *Prog. Theor. Phys.* **103** 151 (2000)
53. Van Kampen N G *Phys. Rep.* **24** 171 (1976)
54. Van Kampen N G *Physica* **74** 239 (1974)
55. Simonov Yu A, in *QCD*: *Perturbative or Nonperturbative*?: *Proc. of the XVII Autumn School, Lisbon, Portugal, 24 Sept.–4 Oct. 1999* (Eds L S Ferreira, P Nogueira, J I Silva-Marcos) (Singapore: World Scientific, 2000); hep-ph/9911237
56. Eidemüller M, Jamin M *Phys. Lett. B* **416** 415 (1998)
57. Shevchenko V I, hep-ph/9802274
58. Shevchenko V I, Simonov Yu A *Phys. Lett. B* **437** 131 (1998)
59. Mandelstam S *Phys. Rev.* **175** 1580 (1968)
60. Simonov Yu A *Phys. Lett. B* **464** 265 (1999)
61. Antonov D V *Yad. Fiz.* **60** 553 (1997) [*Phys. Atom. Nucl.* **60** 478 (1997)]
62. Campostrini M, Di Giacomo A, Mussardo G *Z. Phys. C*: *Part. Fields* **25** 173 (1984)
63. Campostrini M, Di Giacomo A, Olejnik S *Z. Phys. C*: *Part. Fields* **34** 577 (1986)
64. Campostrini M et al. *Phys. Lett. B* **225** 403 (1989)
65. Di Giacomo A, Panagopoulos H *Phys. Lett. B* **285** 133 (1992)
66. Di Giacomo A, Meggiolaro E, Panagopoulos H *Nucl. Phys. B* **483** 371 (1997)
67. Shevchenko V, Simonov Yu *Phys. Rev. D* **65** 074029 (2002)
68. Bali G S *Nucl. Phys. B*: *Proc. Suppl.* **83** 422 (2000)
69. Bali G S *Phys. Rev. D* **62** 114503 (2000)
70. Deldar S *Phys. Rev. D* **62** 034509 (2000)
71. Deldar S *Nucl. Phys. B*: *Proc. Suppl.* **73** 587 (1999)
72. Del Debbio L et al. *Phys. Rev. D* **65** 021501 (2002)
73. Del Debbio L et al. *JHEP* **0201** 009 (2002)
74. Lucini B, Teper M *Phys. Lett. B* **501** 128 (2001)
75. Lucini B, Teper M *Phys. Rev. D* **64** 105019 (2001)
76. Ambjørn J, Olesen P, Peterson C *Nucl. Phys. B* **240** 189, 533 (1984)
77. Simonov Yu A *Pis'ma Zh. Eksp. Teor. Fiz.* **71** 187 (2000) [*JETP Lett.* **71** 127 (2000)]
78. Shevchenko V, Simonov Yu *Phys. Rev. Lett.* **85** 1811 (2000)
79. Trottier H D *Phys. Lett. B* **357** 193 (1995)
80. Lee K *Phys. Rev. D* **48** 2493 (1993)
81. Antonov D V *Surv. High Energ. Phys.* **14** 265 (2000)
82. Antonov D *JHEP* **0007** 055 (2000)
83. Nachtmann O, in *Workshop on Nuclear Chromodynamics — Quarks and Gluons in Particles and Nuclei, Santa Barbara, Calif., USA, 12–23 Aug. 1985* (Eds S Brodsky, E Moniz) (Singapore: World Scientific, 1986) p. 183
84. Simonov Yu A, in *Proc. of the 3rd Intern. Sakharov Conf. on Physics, Moscow, June 24–29, 2002* (Ed. A Semikhatov) (Moscow, 2003)
85. Simonov Yu A, Molodtsov S V *Pis'ma Zh. Eksp. Teor. Fiz.* **60** 230 (1994) [*JETP Lett.* **60** 240 (1994)]
86. Kuz'menko D S *Yad. Fiz.* (in press)
87. Simonov Yu A, hep-ph/0011114
88. Simonov Yu A, hep-ph/9911237
89. Shevchenko V I, ITEP-PH-1-98
90. Abrikosov A A *Zh. Eksp. Teor. Fiz.* **32** 1442 (1957) [*Sov. Phys. JETP* **5** 1174 (1957)]
91. Nielsen H B, Olesen P *Nucl. Phys. B* **61** 45 (1973)
92. Nambu Y *Phys. Rev. D* **10** 4262 (1974)
93. Lifshitz E M, Pitaevskiĭ L P *Statisticheskaya Fizika* (Statistical Physics) Pt. 2 (Moscow: Fizmatlit, 2000) [Translated into English (Oxford: Pergamon Press, 1980)]
94. Landau L D, Lifshitz E M *Elektrodinamika Sploshnykh Sred* (Electrodynamics of Continuous Media) (Moscow: Nauka, 1982) [Translated into English (Oxford: Pergamon Press, 1984)]
95. Badalian A M, Kuzmenko D S *Phys. Rev. D* **65** 016004 (2002)
96. Badalian A M, Kuzmenko D S, in *NPD-2002 Conf., Moscow, ITEP, Dec. 2–6, 2002*; hep-ph/0302072
97. Bali G S, Schlichter C, Schilling K *Prog. Theor. Phys. Suppl.* (131) 645 (1998)
98. Kuzmenko D S, Simonov Yu A *Yad. Fiz.* **66** 983 (2003) [*Phys. Atom. Nucl.* **66** 950 (2003)]; hep-ph/0202277
99. Simonov Yu A, in *Perturbative and Nonperturbative Aspects of Quantum Field Theory* (Lecture Notes in Physics, Vol. 479, Eds H Latal, W Schweiger) (Berlin: Springer, 1997) p. 139
100. Simonov Yu A *Yad. Fiz.* **58** 113 (1995) [*Phys. Atom. Nucl.* **58** 107 (1995)]
101. Feynman R P *Phys. Rev.* **80** 440 (1950); **84** 108 (1951)
102. Fock V A *Izv. Akad. Nauk SSSR Otd. Mat. Estestv. Nauk* 557 (1937)
103. Schwinger J *Phys. Rev.* **82** 664 (1951)
104. Kuzmenko D S *Yad. Fiz.* (in press); hep-ph/0204250
105. Takahashi T T et al. *Phys. Rev. D* **65** 114509 (2002)
106. Alexandrou C, de Forcrand Ph, Jahn O, hep-lat/0209062